



JAIST International Symposium on Nano-Materials for Novel Devices

ABSTRACT

January
11 (Thu) – 12 (Fri) 2024



Co-organized by KAKENHI 2.5 Dimensional Materials Research Area and JSAP Hokuriku Shinetsu Chapter
Partially subsidized by Nippon Sheet Glass Foundation for Materials Science and Engineering (NSG Foundation).

Greeting

Fundamental technologies for the development of innovative devices that transcend conventional semiconductor devices have become an important strategic goal. Currently, countries are competing to develop nanoscale semiconductor devices as a national strategy, but such development require the establishment of technological foundations and scientific principles that transcend conventional semiconductor devices, such as the search for novel functions brought about by the low dimensionality and quantum nature latent in the nanoscale and the elucidation of the physical and chemical mechanisms involved in controlling such functions. In particular, two-dimensional materials are expected to be ideal materials that respond to the miniaturization, low power consumption, and high speed of devices, and their importance is being recognized.

This symposium will be held in the hope that researchers active in this field will present their topics as invited talk and new ideas and discoveries will emerge from cross-talking among all participants. We also expect that young researchers and students will be able to make further progress through exchanges with senior researchers.



大島 義文

Professor Yoshifumi Oshima

Chair of the Organizing Committee
Director, Nanomaterials and Devices Research Area
Japan Advanced Institute of Science and Technology

Time Schedule

11th, January, 2024

- 12:00 Open
12:30 Reception (desk) Open
- 13:00 Welcome Speech (Prof. Minoru TERANO, President of JAIST)
13:10 **Prof. Jana Vejpravova** (Keynote lecture1)
"Prospects of chiral light-matter interaction in van der Waals materials"
13:50 **Prof. Hiroki Ago** (Invited talk, Domestic1)
"Large-scale growth and integration of high-quality 2D materials for 2.5D materials science"
14:20 **Prof. Yukiko Yamada-Takamura** (Invited talk, JAIST1)
"Novel 2D Materials Beyond Graphene Stabilized on Substrates"
- 14:50 Break
- 15:20 **Assoc. Prof. Goki Eda** (Keynote lecture2)
"Engineering 2D Semiconductors for Quantum Photonics"
16:00 **Prof. Kohsuke Nagashio** (Invited talk, Domestic2)
"Shift current photovoltaics in in-plane ferroelectric SnS"
16:30 **Prof. Hiroshi Mizuta** (Invited talk, JAIST2)
"Downscaled Graphene Devices for Advanced Sensing and Thermal Engineering"
- 17:00 Group Photo
17:10 Break
- 17:30 Night session 1
Brief Introduction (1 mins) of Poster presenters
18:30 Night session 2 (Poster and Dinner)
20:00 Special talk
Prof. Martin Kalbac (J. Heyrovsky Institute of Physical Chemistry)
"Introduction to the Advanced Multiscale Materials for Key Enabling Technologies (AMULET) project"
Prof. Guy Le Lay (Aix-Marseille University),
"Of Frogs and Men: Ig Nobel Prize, Scotch Tape, and Sir Andre Geim"
- 21:00 Session close

12th, January, 2024

9:00 Open

10:00 **Dr. Jerzy T. Sadowski** (Keynote lecture3)

"Electron Spectro-Microscopy of 2D Materials and Devices"

10:40 **Assoc. Prof. Yoshiomi Hiranaga** (Invited talk, Domestic3)

"Visualization of nanoscale ferroelectric domain dynamics based on local capacitance measurements"

11:10 **Prof. Eisuke Tokumitsu** (Invited talk, JAIST3)

"Fabrication of oxide and transition metal dichalcogenide films by solution process for thin film transistor applications"

11:40 NMND Young researchers Award and Closing remark

12:00 End

Introduction of invited speaker



Prof. Jana Vejpravova

Department of Condensed Matter Physics,
Charles University, Prague, CZ

Main field: magnetism, condensed matter, physics, low-temperature physics, nanomaterials

<https://www.tsunamigroup.eu/member/jana-vejpravova/>



Assoc. Prof. Goki Eda

Faculty of Science,
National University of Singapore

Main field: Exciton optoelectronics, Quantum charge transport, Novel synthesis of 2D crystals

<https://chemistry.nus.edu.sg/people/goki-eda/>



Dr. Jerzy T. Sadowski

Staff Scientist, Interface Science and Catalysis Group,
Center for Functional Nanomaterials, Brookhaven National Laboratory

Main field: Surface and interface science, thin film growth, surface morphology and crystallinity, surface chemistry and electronic structure, catalytic properties, 2D van der Waals materials, thin films and heterostructures, Elemental 2D materials – graphene and beyond

<https://www.bnl.gov/staff/sadowski>



Prof. Hiroki Ago

Global Innovation Center (GIC), Kyushu University

Main field: carbon electronics, graphene, metal dichalcogenides, atomic sheet, carbon nanotubes, crystal growth, CVD, nanotechnology, transistors, molecular electronics

<https://www.gic.kyushu-u.ac.jp/ago/selfintro-e.html>



Prof. Kohsuke Nagashio

Department of Materials Engineering, The University of Tokyo

Main field: 2D materials, layered heterostructure, electronic transport properties, crystal growth

https://www.material.t.u-tokyo.ac.jp/faculty/kosuke_nagashio_e.html



Assoc. Prof. Yoshiomi Hiranaga

Research Institute of Electrical Communication, Tohoku University

Main field: scanning nonlinear dielectric microscopy. ferroelectric materials, electronic devices

https://www.d-nanodev.riec.tohoku.ac.jp/english/subcontents/contents_301.html



Prof. Yukiko Yamada-Takamura

Nanomaterials and devices researcher area, JAIST

Main field: nanomaterials, 2D materials, thin films, ultra-high vacuum, hetero-epitaxial growth, surface and interfaces

<https://www.jaist.ac.jp/english/laboratory/nd/takamura.html>

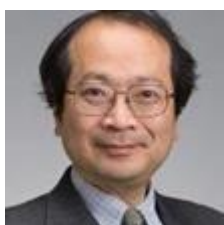


Prof. Hiroshi Mizuta

Sustainable Innovation researcher area, JAIST

Main field: NEMS, single molecular sensing, atom-scale fabrication, quantum devices, ab initio simulation

<https://www.jaist.ac.jp/english/laboratory/si/mizuta.html>)



Prof. Eisuke Tokumitsu

Nanomaterials and devices researcher area, JAIST

Main field: thin film transistor, oxide semiconductor, ferroelectric material, nonvolatile memory

<https://www.jaist.ac.jp/english/laboratory/nd/tokumitsu.html>

Special speaker



Prof. Martin Kalbac

(J. Heyrovsky Institute of Physical Chemistry)



Prof. Guy Le Lay

(Aix-Marseille University)

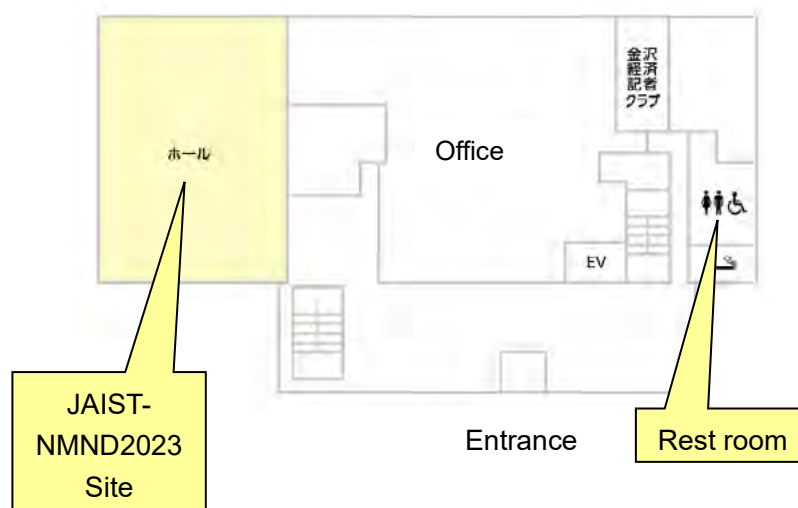
Requests for Poster Presenters

- (1) The maximum poster size is **A0 (Vertically long)**.
- (2) Prepare a PowerPoint presentation to introduce your presentation in oral (1 minute).
- (3) The room will open at 12:00 on January 11.
- (4) We would like to receive the file of your PowerPoint presentation at the registration desk. This file will be erased after the symposium.
- (5) We will provide "studs" to display your poster. Please post your poster at your poster number.
- (6) Please take down your posters on the morning of January 12.

Venue Information

- (1) Coffee, tea, green tea, water, and hot water are available.
- (2) WIFI is available at the venue free of charge.
SSID: Kanazawa_cci_a or Kanazawa_cci_g
Pass: 0762631151
- (3) Maps (in English) of the area around the venue are available at the registration desk, so please feel free to bring your own.

You can view travel guides of Kanazawa in PDF here.
<https://visitkanazawa.jp/en/pamphlet/index.html>



Poster Presentation

A: Structure & Growth,

B: Methodology & Characterization,

C: Physical properties & Functions

- A-01: **XU, Yuanzhe** (JAIST) "Study of structural features of Kanazawa gold leaves"
- A-02: **CHADIZA, Nadia Maharani** (Kanazawa University) "First-principles study of the van der Waals ZnO layers"
- A-03: **HASAN, Wakil** (Kobe University) "Density functional study of VO₂ growth on hexagonal boron nitride & graphene"
- A-04: **MATSUYAMA, Keigo** (The University of Tokyo) "Phase Conversion to the Air-stable 1T'-MoS₂ by a Chemical Procedure"
- A-05: **MORIYAMA, Akihide** (Kanazawa University) "Atomic Study of MBE-grown Mn Thin Films on Insulating Substrates"
- A-06: **WISESA, Sulthan Waliid Anggara** (Kanazawa University) "A first-principles study of hydrogen and oxygen adsorption in mercury iodide HgI₂ monolayer"
- A-07: **SUZUKI, Seiya** (Japan Atomic Energy Agency) "Repeatable growth of segregated germanene by oxidation and reheating"
- A-08: **YOKOO, Takato** (JAIST) "Research on Ultrathin Sn Films Grown on InSb(111)A for the Growth of Stanene"
- A-09: **ISLAM, Md Tauhidul** (JAIST) "Influence of InAs thickness on surface morphology in low-temperature grown MnAs/InAs/MnAs double heterostructure on GaAs (111)B"
- A-10: **GELAN, Jieensi** (JAIST) "Wet etching of AlGa_N via removal of altered layer obtained by Ti-AlGa_N reaction"
- A-11: **KABIR, Md Faysal** (JAIST) "MnSb and InSb grown on GaAs (111)B for spin-FET application"
- B-01: **OGAWA, Tomoya** (Tokyo Metropolitan University) "Synthesis and optical properties of high-quality monolayer Janus MoSSe on hBN substrates"
- B-02: **NAGANO, Tatsuki** (JAIST) "Focusing Optics to Improve Beam Spot Properties at the XPEEM/LEEM Endstation of the ESM beamline at the NSLS-II"
- B-03: **MAMIYA, Ryota** (JAIST) "Observation saccharides distribution in rice grains by Sum Frequency Generation confocal microscopy"
- B-04: **TSUJIMURA, Kohei** (JAIST) "Observation before and after addition of trivalent metal ions to SACRAN cast films using femtosecond laser SHG microscopy"
- B-05: **MAN, Erlina Tik** (Kanazawa University) "Development of a Cryogenic High Magnetic Field Scanning Tunneling Microscope Integrated with Microwave Irradiation Capability"
- B-06: **NAKANO, Yohei** (Kanazawa University) "Structural and chemical analysis of tungsten tips for scanning probe microscopy prepared by flame etching"
- B-07: **MATSUURA, Gosuke** (Kobe University) "Simulation of harmonic generation in silicon nanocylinder"
- B-08: **PRANANTO, Dwi** (JAIST) "Coherence Properties Improvement of Scanning Diamond Quantum Probes Fabricated by Ga⁺ Focused Ion Beam"

- B-09: **WANG, Yifei** (JAIST) "Optimization of scanning diamond NV center probes fabricated by using FIB"
- B-10: **AOKI, Yuma** (JAIST) "Fabrication of scanning diamond NV center quantum sensing probes by using maskless photolithography"
- B-11: **NODA, Kasane** (JAIST) "Optimization of spin properties of near-surface NV centers in diamond"
- B-12: **ASO, Kohei** (JAIST) "Three-dimensional atomic-scale structural characterization of titanium oxyhydroxide nanoparticles by statistical electron microscopy analysis"
- B-13: **UEMOTO, Mitsuharu** (Kobe University) "First-principles study on structural and electronic properties of FePd/graphene hetero-interfaces"
- B-14: **UNO, Atsuki** (JAIST) "Introduction of microscopic nanomechanical measurement method"
- B-15: **LIU, Jiaming** (JAIST) "Estimation of Critical Shear Stress of Au nanocontacts using microscopic nanomechanics measurement method"
- C-01: **EMOTO, Satoru** (Kyushu University) "Application of large-area CVD-grown few-layer hexagonal boron nitride to magnetic tunnel junction devices"
- C-02: **TEWENG, Yedija Yusua Sibuea** (Kanazawa University) "First-principles study on bulk photovoltaic effect in topological insulator phase of halide perovskites"
- C-03: **JUNG, Eui Young** (Kyushu University) "Transferable high-k/boron nitride gate dielectric for 2D field-effect transistors"
- C-04: **SHIMOKAWA, Takaya** (Kanazawa University) "Enhanced superconductivity by intrinsic strain in NbTe₂"
- C-05: **XIONG, Wei** (JAIST) "Precise measurement of ripple structure of MoS₂ nanoribbon when stretching"
- C-06: **CHEN, Limi** (JAIST) "Electrical conductance of suspended MoS₂ nanoribbon measured by in-situ transmission electron microscope"
- C-07: **NAKASHIMA, Mai** (JAIST) "In-situ TEM observation of effect of electron irradiation on electrical conductance in GaSe films"
- C-08: **MIYATA, Hirohisa** (JAIST) "Electron trap prediction based on solid-state electronic structure for lanthanide ions doped CaCO₃ phosphors"
- C-09: **GAS-OSOTH, Thitinun** (JAIST) "Double Electron-Electron Resonance Spectroscopy by Using a Scanning Nitrogen Vacancy Center Diamond Probe"
- C-10: **HAYASHI, Kunitaka** (JAIST) "Temperature detection using a scanning diamond NV center probe for thermal imaging "
- C-11: **FATOMI, Zohan Syah** (Kanazawa University) "First Principles Study of Electron and Phonon in BaSi₂ Polymorph"
- C-12: **FAUZI, Akmal** (Kanazawa University) "Application of Machine Learning in High-Throughput Screening of 2D Materials for Transverse Thermoelectric"
- C-13: **KAKEYA, Takafumi** (JAIST) "Electron microscopy study of Zr oxides coating effect on charge-discharge properties of LiCoO₂ cathode for lithium-ion batteries"
- C-14: **WICAKSONO, Yusuf** (RIKEN) "Enhancing Rashba Spin-Orbit Coupling by Engineering Superlattice Interfaces of Light-Element Metal"
- C-15: **CUNJIAN, Lin** (JAIST) "Enabling visible-light-charged near-infrared persistent luminescence in organics by intermolecular charge transfer"

Abstract
Invited talk

Prospects of chiral light-matter interaction in van der Waals materials

Jana K. Vejpravova

Charles University, Faculty of Mathematics and Physics, Ke Karlovu 5, 121 16 Prague 2, Czech Republic

Van der Waals (vdW) materials and their heterostructures feature significant electronic and optical properties tunable via external physical fields (photonic, magnetic, electric, and strain) or proximity effects with other materials and molecules, which made them superior constituents for advanced optoelectronic/spintronic devices. The Raman (Ra) and photoluminescence (PL) micro-spectroscopies are eminent tools for exploring electronic, optical, and spin phenomena in vdW materials and their heterostructures [1-4]. By employing light with intrinsic helicity, the valley physics and magnetic order are accessible thanks to the selective valley excitation and spin-lattice coupling, respectively [5, 6]. Also, various proximity effects can be explored in the individual layers of the hybrid heterostructures. In this talk, selected results obtained on hybrid layered architectures based on transition metal dichalcogenides, layered magnets, and magnetic molecules, including their rational design, fabrication, and performance under chiral light and magnetic field down to helium temperatures, will be presented.

[1] Haider G., Sampathkumar K., Verhagen T., Nádvorník L., Sonia F. J., Vales V., Sykora J., Kapusta P., Nemeč P., Hof M., Frank O., Chen Y.-F., Vejpravova J., Kalbac M., *Adv. Funct. Mater.* (2021) 2102196.

[2] Verhagen T., Klimes J., Pacakova B., Kalbac M., Vejpravova J., *ACS Nano* 14, 15587-15594(2020).

[3] Verhagen T., Guerra V. L. P., Golam H., Kalbac M., Vejpravova J., *Nanoscale* 12, 3019 – 3028 (2020)

[4] Verhagen T., Drogowska K., Kalbac M., Vejpravova J., *Physical Review B* 92, 125437 (2015).

[5] V. Varade, G. Holam, A. Slobodeniuk, R. Korytar, T. Novotny, V. Holy, J. Plsek, M. Zacek, M. Basova, J. Sykora, M. Hoff, J. Miksatko, M. Kalbac, J. Vejpravova, *ACS Nano* 17, 2170 (2023).

[6] Ghosh, A., Singh D., Mu Q., Kvashnin Y., Haider G., Jonak M., Chareev D., Aramaki T., Medvedev S.A., Klingeler R., Mito M., Abdul-Hafidh E.H., Vejpravova J., Kalbac M., Ahuja R., Eriksson O., Abdel-Hafiezar M., *Phys. Rev. B* 105, L081104, (2022) (Editors' Suggestion)

Biography

JKV is a full professor and group leader at the Department of Condensed Matter Physics, Faculty of Mathematics and Physics at Charles University, Prague. She graduated from Charles University with MSc. in "Chemistry" in 2003 and a Ph.D. in "Condensed Matter Physics and Materials Research" in 2007. After her postdoctoral stays at Hasselt University, Belgium, and the National Institute for Materials Science, Tsukuba, Japan, she worked as the head of the department at the Institute of Physics, Czech Academy of Sciences (2011–2017). Her current research interests cover the experimental physics of low-dimensional materials, including carbon nanotubes, magnetic nanoparticles, graphene, and other two-dimensional materials, focusing on advanced magnetometry techniques, cryomagnetic optical, and nuclear spectroscopies. She also has ~20 years of experience in neutron and synchrotron radiation scattering techniques applied to magnetic materials and nanomaterials. Her work has been funded by ~20 projects as PI (~8 MEUR), including the prestigious ERC Starting grant (2016). Among her important responsibilities are memberships in the expert panel for the Graphene Flagship monitoring and the expert panel of the Research, Development, and Innovation Council. She published ~170 papers, presented ~30 invited/plenary talks, and received multiple recognitions, e.g., Scopus/Elsevier Award (2010), Otto Wichterle Award (2014), F. Behounek Award for promotion and popularization of Czech science in the European Research Area (2019), and recently has been appointed as one of the top female research in Czechia by FORBES (2023).

Large-scale growth and integration of high-quality 2D materials for 2.5D materials science

Hiroki Ago

Global Innovation Center (GIC), Kyushu University, Fukuoka, Japan
Interdisciplinary Graduate School of Engineering Sciences, Kyushu University, Fukuoka, Japan

Since the discovery of graphene, two-dimensional (2D) materials have been intensively studied because of their unique physical properties and various applications. The integration of 2D materials and other low dimensional materials offers new opportunities to explore a field of materials science, in terms of synthesis of new materials and observation of new phenomena based on van der Waals (vdW) interaction as well as utilization of vdW nanospace. We expect that such new research direction can be further developed based on a new concept of "Science of 2.5D materials", as illustrated in Figure 1.

In this presentation, our recent research based on the 2.5D concept will be introduced, first showing the controlled CVD growth of bilayer graphene (BLG) and machine learning-based twist angle determination [1,2]. The 2D nanospace in BLG was used to intercalate metal chloride molecules and alkaline metals, revealing new unique 2D structures as well as significant reduction of the sheet resistance of BLG, strongly depending on twist angles [3-5]. We have also developed the CVD growth of high-quality, multilayer hBN (Figure 2) to be used as a building block of various 2.5D materials, such as graphene field transistors (FETs) [6-8]. The generation of 2.5D materials will open a new research field enriched with fascinating properties and promising applications. I will also introduce our new result of tape transfer of 2D materials, which is expected to accelerate the 2D/2.5D materials research.

Finally, our group research project, "Science of 2.5 Dimensional Materials: Paradigm Shift of Materials Science Toward Future Social Innovation" supported by MEXT, Japan will be also introduced in my presentation [9,10].

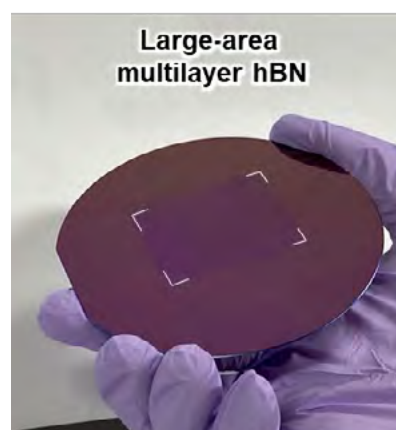
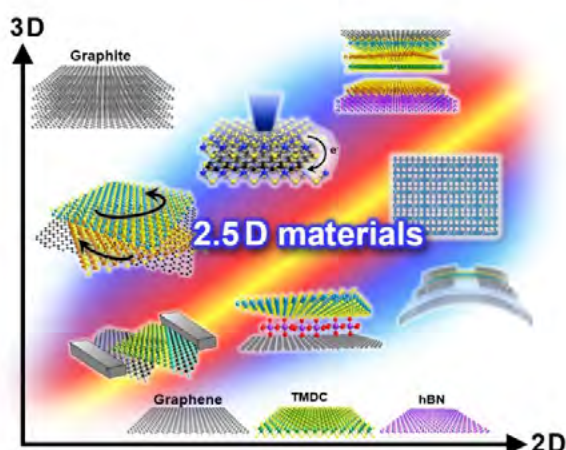


Fig. 1. Concept of "Science of 2.5D materials" [9,10]. **Fig. 2.** Transferred large multilayer hBN [7].

References:

- [1] P. Solís-Fernández et al., *ACS Nano*, **14**, 6834 (2020). [2] P. Solís-Fernández et al., *ACS Appl. Nano Mater.*, **5**, 1356-1366 (2022). [3] Y.-C. Lin et al., *Adv. Mater.*, **33**, 2105898 (2021). [4] Y. Araki et al., *ACS Nano*, **16**, 14075 (2022). [5] Y.-C. Lin et al., *Nat. Commun.*, in press. [6] Y. Uchida et al., *ACS Nano*, **12**, 6236 (2018). [7] Y. Uchida et al., *ACS Appl. Electron. Mater.*, **2**, 3270 (2020). [8] S. Fukamachi et al., *Nat. Electron.*, **6**, 126 (2023). [9] M. Nakatani et al., *Nat. Electron.* in revision. [10] H. Ago et al., *Sci. Tech. Adv. Mater.*, **23**, 275 (2022). [10] <https://25d-materials.jp/en/>

Novel 2D Materials Beyond Graphene Stabilized on Substrates

Yukiko Yamada-Takamura

School of Materials Science, Japan Advanced Institute of Science and Technology (JAIST), Japan.

One way to realize novel two-dimensional (2D) materials which lack “layered host materials” is to grow them epitaxially on single-crystalline substrates. Such materials have to be characterized by complementary methods, and first-principles calculation is necessary to understand their crystal and electronic structures. Here in JAIST, our group has been working on a variety of such materials by collaborating with other groups in the world having complementary expertise.

The first example is “silicene”, a Si-version graphene, having honeycomb structure. We have demonstrated, in 2012, by a combination of scanning tunnelling spectroscopy (STM), core-level and angle-resolved photoelectron spectroscopy (ARPES), and first-principles electronic structure calculations, that on epitaxial $\text{ZrB}_2(0001)$ films grown on Si(111) substrates, Si atoms segregate to the film surface and crystallize in a honeycomb structure having stripe domains [1,2]. Although this silicene sheet is vulnerable against oxygen in air, it can be protected by “white graphene”. Through nitridation of $\text{ZrB}_2(0001)$ film surface in ultrahigh vacuum, it is possible to form a hBN monolayer on film surface, and by exposing this surface to Si vapor, Si atoms intercalate inbetween hBN monolayer and $\text{ZrB}_2(0001)$ film surface forming silicene protected by an insulating atom-thick layer [3].

The second example is a 2D Ge lattice having a “bitriangular” structure. Our theoretical study on freestanding bitriangular lattice demonstrated that the flat band of a kagome lattice can be embedded in this very different structure [4]. In parallel, we have grown $\text{ZrB}_2(0001)$ thin films on Ge(111) substrates, and by combing STM, total reflection high energy positron diffraction, photoelectron spectroscopy, and first-principles calculations, we found that Ge atoms segregate and crystallize into such a bitriangular lattice on the ZrB_2 film surface [5]. The electronic structure measured by ARPES reveals “nearly” flat band at room temperature.

The third example is a new polymorph of monolayer GaSe which is a semiconducting monochalcogenide. Bulk GaSe is known to crystallize in four “polytypes” which differ in how layers are stacked via van der Waals interaction, but no “polymorph” has been reported based on experimental study, including other layered monochalcogenides with the same crystal structure, such as GaS and InSe. Through detailed cross-sectional scanning transmission electron microscopy of GaSe thin films grown on Ge(111) substrates, we found that monolayer GaSe with “trigonal anti-prismatic structure”, which is a new polymorph, exist near the film-substrate interface [6]. Our first-principles study implies that the new phase is a metastable phase and can be stabilized under tensile strain [7].

These are a few examples of 2D materials stabilized on substrates recognized for the first time through careful investigations.

References:

- [1] A. Fleurence, R. Friedlein, T. Ozaki, H. Kawai, Y. Wang, and Y. Yamada-Takamura, *Phys. Rev. Lett.* **108**, 245501 (2012).
- [2] Y. Yamada-Takamura and R. Friedlein, *Sci. Technol. Adv. Mater.* **15**, 064404 (2014).
- [3] F. B. Wiggers, *et al.*, *2D Materials* **6**, 035001 (2019).
- [4] C.-C. Lee, A. Fleurence, Y. Yamada-Takamura, and T. Ozaki, *Phys. Rev. B* **100**, 045150 (2019).
- [5] A. Fleurence *et al.*, *Phys. Rev. B* **95**, 201102(R) (2020).
- [6] T. Yonezawa, T. Murakami, K. Higashimine, A. Fleurence, Y. Oshima, and Y. Yamada-Takamura, *Surf. Interface Anal.* **51**, 95-99 (2019).
- [7] H. Nitta, T. Yonezawa, A. Fleurence, Y. Yamada-Takamura, and T. Ozaki, *Phys. Rev. B* **102**, 235407 (2020).

Engineering 2D Semiconductors for Quantum Photonics

Goki Eda^{1,2,3}¹ Department of Physics, National University of Singapore, Singapore 117551² Department of Chemistry, National University of Singapore, Singapore 117543³ Centre for Advanced 2D Materials, National University of Singapore, Singapore 117546E-mail: g.eda@nus.edu.sg; Website: <http://phyweb.physics.nus.edu.sg/~phyeda/>

Atomic defects in semiconductors are an attractive building block for solid-state quantum technology. In 2015, defects in two-dimensional (2D) semiconductors such as monolayer WSe₂ were found to exhibit single photon emission, attracting great attention as promising candidates in quantum photonic devices. These 2D semiconductors, characterized by strong excitonic effects, are expected to host a variety of defect-bound excitons that are rich in physics, inheriting the unique properties of the host crystal. However, the structural and physical origin of bound excitons remains elusive, hindering strategic defect engineering. I will first discuss controlled in-situ and ex-situ generation of atomic defects in the dilute limit where quantum effects are expected [1, 2]. I will then discuss determination of the many-body nature of bound excitons through electro- and magneto-optical spectroscopy [2,3]. Finally, I will discuss our findings on single atomic defect conductivity and photoconductivity, demonstrating an innovative method for rapid and precise quantification of select impurities in the dilute limit ($<10^{10}$ cm⁻²) under ambient condition [4].

[1] Loh et al. "Impurity-induced emission in Re-doped WS₂ monolayers" *Nano Lett.* 21, 5293 (2021).

[2] Loh et al. "Dilute acceptor-bound excitons in monolayer semiconductor" Under review.

[3] Chen et al. "Gate-tunable bound exciton manifolds in monolayer MoSe₂" *Nano Lett.* 23, 4456 (2023).

[4] Nam et al. "Single atomic point defect conductivity for dilute impurities imaging in 2D semiconductors" *ACS Nano*, 17, 15648 (2023).

Short biography: Dr. Eda is Associate Professor of Physics and Chemistry at the National University of Singapore, and a member of the Centre for Advanced 2D Materials (CA2DM). Before joining NUS in 2021, he was a Newton International Fellow of the Royal Society of the UK and worked at Imperial College London. Dr. Eda received his M.Sc. in Materials Science and Engineering from Worcester Polytechnic Institute in 2006 and Ph.D. in the same discipline from Rutgers University in 2009. He is a recipient of the Singapore National Research Foundation (NRF) Research Fellowship and many awards including the Singapore National Academy of Science (SNAS) Young Scientist Award and University Young Researcher Award. He is an Associate Editor of *npj 2D Materials and Applications*. His research focuses on the electronic, photonic, and magnetic device physics of two-dimensional materials.

Shift current photovoltaics in in-plane ferroelectric SnS

Kosuke Nagashio

Materials Engineering, The University of Tokyo, JAPAN
nagashio@material.t.u-tokyo.ac.jp

Lack of inversion symmetry give birth to a variety of functionalities. For example, the spontaneous photovoltaic effect, so called shift current, is one of the fascinating properties. However, its conversion efficiency has been largely limited so far in the conventional material systems. Here, monolayer SnS is predicted to show high shift current tensor comparable to Si based solar cell, which attracts the intensive research [1]. Although a strain-stabilized non-centrosymmetric phase, β' phase, of SnS was grown on mica substrate and its ferroelectricity was demonstrated [2], the crystallinity is still not high enough. By introducing the van der Waals substrate in PVD growth of SnS, the crystallinity was drastically improved. Taking advantage of this high-quality β' phase, the bulk photovoltaic effect of SnS is explored in this research, as shown in Fig. 1.

To prove the existence of shift current, another spontaneous photovoltaic effect resulted from built-in potential formed at the Schottky junction should be separated from the shift current generated from non-centrosymmetric structure. The key feature here is two SnS flakes linked with each other in armchair direction for longer device channel length, as shown in Fig. 2. In addition, Al covers are deposited on h-BN protection layer at contact electrode regions to suppress the photocurrent resulted from Schottky junction.

Followed by the photocurrent scanning along the channel region of SnS device using 488-nm laser, four photocurrent peaks can be clearly distinguished, as shown in Fig. 3. It can be found that peaks 1 & 4 are located at the edges of electrode contacts and should result from the Schottky junction. Meanwhile, peaks 2 & 3 are located at the channel region of the device, which indicates that they are contributed by shift current of SnS. Moreover, as shown in Fig. 4, the polarized pattern with its polarization direction in good agreement with SnS flake orientation is a robust evidence of shift current observation.

The shift current of SnS is confirmed and analyzed [3]. The results obtained here can serve as a milestone for the future development of shift current photovoltaic devices based on 2D materials.

References:

- [1] T. Rangel et al., PRL, 2017, 119, 067402.
- [2] N. Higashitarumizu, et al., Nat. Commun., 2020, 11, 2428.
- [3] Y.-R. Chang, et al., Adv. Mater., 2023, 35, 2301172.

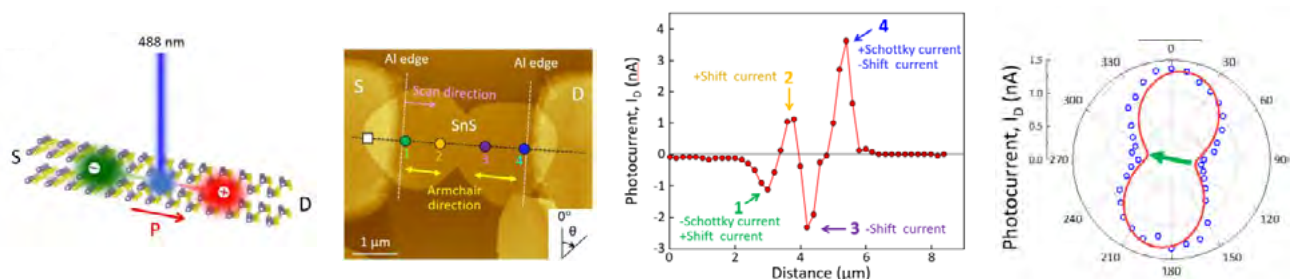


Fig. 1 Shift current generation.

Fig. 2 AFM image of SnS.

Fig. 3 Photocurrent along dotted line.

Fig. 4 Polarized dependence.

Downscaled Graphene Devices for Advanced Sensing and Thermal Engineering

Hiroshi Mizuta^{1,2}, Afsal Kareekunnan¹, and Manoharan Muruganathan¹,

¹ Sustainable Innovation Research Area, Japan Advanced Institute of Science and Technology, JAPAN.

² School of Electronics and Computer Science, University of Southampton, UK.

An overview is presented for our recent study of graphene nanodevices for various challenging applications. Graphene nano-electro-mechanical (GNEM) device technology is first presented for low-power switching and ultra-sensitive chemical gas sensing applications. Three-terminal GNEM switches with heterogeneously stacked graphene / h-BN layers are developed [1], which achieve low-voltage and sub-thermal switching ($S \ll 60$ mV/dec). We then present nanoscale graphene chemical sensors, which detect either resistance or mass changes due to a small number of gas molecules physisorbed onto suspended graphene at room temperature. With the resistance detection method, we show quantized increments in the temporal resistance, signifying individual CO₂ molecule adsorption (Fig. 1(a)) [2]. As for the mass detection method, we demonstrate the resonance frequency shift of a doubly-clamped graphene resonator with the mass resolution of hundreds zeptogram (10^{-21} g) order [3].

In addition, we present our recent attempts of applying graphene nanosensors to detect a variety of faint signals from nature (we describe them as "Silent Voice"). This includes detection of very low concentration skin gas such as NH₃ down to ppt (parts-per-trillion) level [4] in concentration for pre-symptomatic disease detection. We are also making an attempt to sense very low electric field (< 100 V/m) in the atmosphere [5] to develop novel lightning forecast technology (Fig. 1(b)).

After that, state-of-the-art single-nanometer patterning technology of suspended graphene by using helium ion microscope (HIM) (Fig. 1(c)) is introduced for nanoscale thermal engineering. The graphene phononic crystal (GPnC) structures with sub-10-nm pore diameter are patterned on large-area suspended graphene [6]. A new Differential Thermal Leakage method is introduced to evaluate heat phonon transport in the asymmetric GPnC channels (Fig. 1(d)). Remarkable thermal rectification is presented with the rectification ratio of over 80 % at 150 K and 60 % at 250 K [7] along with preliminary discussion on physical mechanism behind the rectification phenomena.

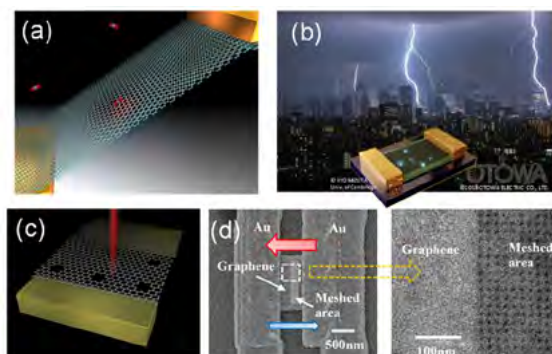


Figure 1 Schematic images of (a) single molecular sensing, (b) lightning sensor, (c) HIM based nanopore patterning, and (d) HIM images of suspended asymmetric GPnC.

References:

- [1] N. H. Van, M. Muruganathan, J. Kulothungan and H. Mizuta, *Nanoscale*, 10 (2018).
- [2] J. Sun, M. Muruganathan, and H. Mizuta, *Science Advances* 2(4), e1501518 (2016)
- [3] M. Muruganathan, F. Seto, and H. Mizuta, *IJAT* 12, 24 (2018) / M. Muruganathan, H. Miyashita, J. Kulothungan, M. Schmidt, H. Mizuta, *IEEE Sensors* 2018, New Delhi, October (2018)
- [4] G. O. Agbonlahor, M. Muruganathan, S. . Ramaraj, Z. Wang, A. Hammam, A. Kareekunnan, H. Maki, M. Hattori, K. Shimomai and H. Mizuta, *ACS Applied Materials & Interfaces* 13, 61770 (2021)
- [5] A. Kareekunnan, T. Agari, A. Hammam, T. Kudo, T. Maruyama, H. Mizuta, and Manoharan Muruganathan *ACS Omega*, 6, 34086-34091(2021)
- [6] M. E. Schmidt, T. Iwasaki, M. Muruganathan, M. Haque, N. H. Van, S. Ogawa and H. Mizuta, *ACS Applied Materials & Interfaces* 10, 10362 (2018)
- [7] F. Liu , M. Muruganathan, Y. Feng, S. Ogawa, Y. Morita, C. Liu, J. Guo, M. Schmidt and H. Mizuta, *Nano Futures* 5(4), 045002 (2021)

Electron Spectro-Microscopy of 2D Materials and Devices

Jerzy T. Sadowski

Center for Functional Nanomaterials, Brookhaven National Laboratory, Upton, NY 11973,
USA

*E-mail: sadowski@bnl.gov

The ongoing miniaturization in technological devices and the progress in surface science demand novel instrumental methods for surface characterization on a length scale of only a few atomic distances. The combination of an x-ray photoelectron emission microscope (XPEEM) or low-energy electron microscope (LEEM) is a powerful technique for studying the dynamic and static properties of 2D materials surfaces and thin films including growth and decay, phase transitions, reactions, surface structure and morphology. It utilizes low energy electrons to image surfaces with few nm lateral resolution and atomic layer depth resolution. In the LEEM/XPEEM setup, when using the electron irradiation, the backscattered electrons, Auger and secondary electrons may be used, while photoelectrons, Auger and secondary electrons are utilized for imaging when sample is irradiated with photons. In this talk I will present examples of the application of the LEEM/XPEEM technique to the investigations of novel materials, including 2D layered materials, thin films, and adsorbate structures.

This research used resources of the Center for Functional Nanomaterials and the National Synchrotron Light Source II, which are U.S. Department of Energy (DOE) Office of Science facilities at Brookhaven National Laboratory, under Contract No. DE-SC0012704.

Visualization of Nanoscale Ferroelectric Domain Dynamics Based on Local Capacitance Measurements

Yoshiomi Hiranaga

Research Institute of Electrical Communication, Tohoku University, Japan.

The key to elucidating various unexplained phenomena of ferroelectric materials and discovering new ones, as well as improving their properties, is to understand the domain dynamics at the nanoscale. Among various microscopy techniques, piezoresponse force microscopy has been widely and commonly used for this purpose. On the other hand, the recently developed local C-V mapping method allows nanoscale analysis of domain dynamics through dielectric rather than piezoelectric measurements. In addition to the difference in the physical phenomena being measured, this method has advantages over PFM-based methods, such as the ability to simultaneously achieve high speed and high sensitivity in observation. Herein, we present a methodology to analyze hyperspectral image data with a huge amount of information generated by this new method using a machine learning approach to extract and visualize the information necessary for understanding domain dynamics. Furthermore, this study focuses on the spatial distribution of the nanoscale polarization switching properties of doped HfO₂ films as a specific application of this methodology. Datasets acquired by the local C-V mapping method were clustered into several regions based on the similarity of their polarization properties using unsupervised learning methods such as k-means and Gaussian mixture model. In addition to the typical butterfly-shaped C-V curves that represent normal polarization inversion, these clusters contained asymmetric butterfly curves that may be caused by domain pinning or other built-in field-derived effects. Subsequent statistical analysis suggested that, in pristine HfO₂ films before wake-up, defects at grain boundaries have some effect on the polarization switching properties, but they are not the main cause of the variation in the properties.

References:

- [1] Y. Hiranaga, T. Mimura, T. Shimizu, H. Funakubo, and Y. Cho, *J. Appl. Phys.* 128, p.244105 (2020).
 [2] Y. Hiranaga, T. Mimura, T. Shimizu, H. Funakubo, and Y. Cho, *Jpn. J. Appl. Phys.* 61, SN1014 (2022).

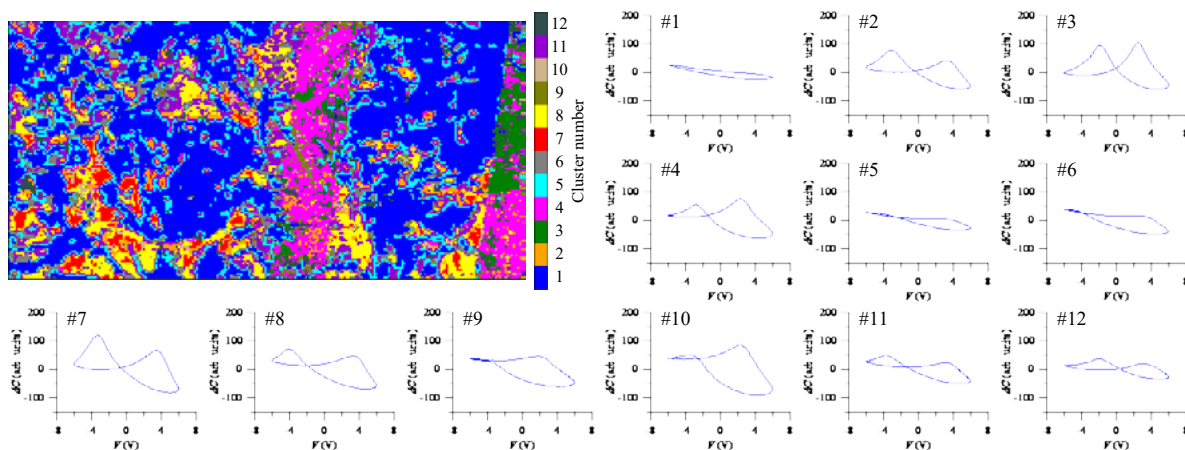


Fig. Example of cluster analysis of a dataset obtained by the local C-V mapping method. Fundamental to thirtieth harmonic SNDM images were acquired with a randomly-oriented HfO₂-based ferroelectric thin film under an AC bias voltage of 12 V_{pp} amplitude. This dataset contained components that enabled the resynthesis of local C-V curves for all 256 × 128 data points in a 4 μm × 2 μm observation area. Dimensionality reduction was performed on this dataset using principal component analysis, followed by cluster analysis based on a Gaussian mixture model. The figure shows a two-dimensional map of the clusters when the number of clusters is set to 12, as well as the averaged C-V curve for each cluster.

Fabrication of oxide and transition metal dichalcogenide films by solution process for thin film transistor applications

Eisuke Tokumitsu,
Japan Advanced Institute of Science and Technology, Japan

Fabrication of semiconducting thin films is one of the key technologies for semiconductor electronics applications, and precise thickness control has been required. Various kinds of techniques are used for this purpose, such as atomic layer deposition (ALD), chemical vapor deposition, molecular beam epitaxy, and sputtering. On the other hand, chemical solution deposition (CSD) is a low cost and low energy consumption thin film preparation process, but the CSD is generally considered unsuitable for fabricating ultra-thin films below 10 nm. In this presentation, our research activities on CSD of oxide and transition metal dichalcogenide (TMDC) ultra-thin films are presented.

Figure 1 shows a cross sectional high-angle annular dark field scanning transmission electron microscope (HAADF-STEM) image of a CeO_x/Y -doped ($\text{Hf,Zr})\text{O}_2$ (Y-HZO)/ CeO_x structure fabricated by CSD with an annealing temperature of 800°C [1]. Thicknesses of CeO_x and HfO_2 layers are 12 and 33 nm, respectively. The clear layered structure was confirmed. We have observed CeO_x layer as thin as 3 nm can be fabricated by CSD. In addition, we have found that the CeO_x , which is a multivalent oxide, can help to form orthorhombic phase of Y-HZO, which results in good ferroelectric properties. Successful n-channel transistor operation with nonvolatile memory function was obtained for the fabricated thin film transistor with an indium-tin-oxide (ITO) channel and $\text{CeO}_x/\text{Y-HZO}$ gate insulator.

We have also demonstrated the fabrication of MoS_2 thin films by CSD technique [2]. For CSD of MoS_2 , sulfurization annealing as high as 1000°C with sulfur powder was performed after the pre-annealing at 450°C in a reduced atmosphere. Figure 2 shows Raman spectra of the MoS_2 films fabricated with various concentrations of the source solution. From the wave number difference between E_{2g} and A_{1g} modes, which can be used for thickness estimation, it is suggested a MoS_2 film as thin as 2-layer can be fabricated by diluting the source solution.

In summary, we have demonstrated the CSD can be a useful tool for fabricating ultra-thin semiconducting films for oxide and TMDC materials.

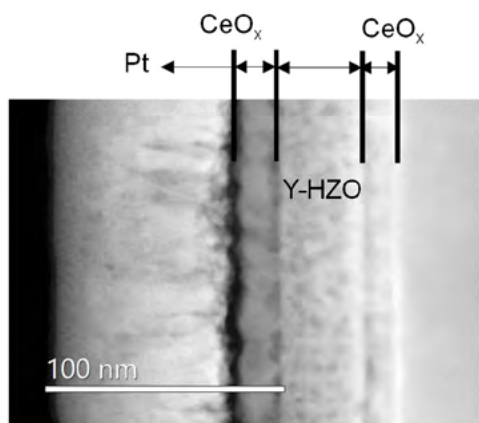


Fig.1 TEM cross section image of $\text{CeO}_x/\text{Y-HZO}/\text{CeO}_x$ layered structure fabricated by CSD [1].

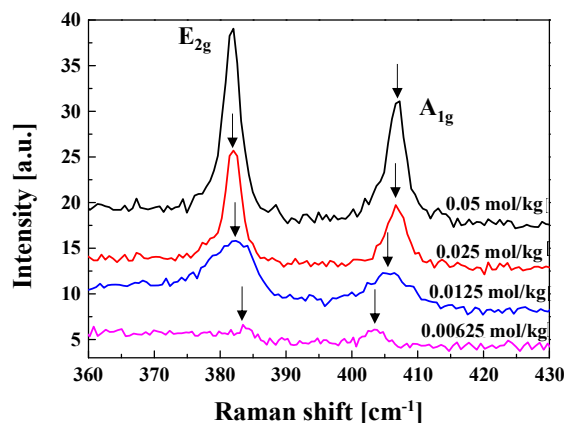


Fig.2 Raman spectra of MoS_2 films fabricated by CSD using various solution concentrations [2].

References:

- [1] M. Saito, Mohit, K. Higashimine, E. Tokumitsu, Jpn. J. Appl. Phys., **63**, 01SP23 (2024).
- [2] J. Kim, K. Higashimine, K. Haga, E. Tokumitsu, Phys. Status Solidi B, **254**, 1600536 (2017).

Abstract

Poster presentation

Study of structural features of Kanazawa gold leaves

Yuanzhe Xu*¹, Kohei Aso¹, Hideyuki Murata¹, Yoshifumi Oshima¹

¹School of Materials Science, Japan Advanced Institute of Science and Technology

*E-mail: s2220019@jaist.ac.jp

In this study, we analyzed the microstructures of Kanazawa gold leaf (composed of 89 at% gold, 8.9 at% silver, and 2.1 at% copper) using Electron Backscatter Diffraction (EBSD) and Transmission Electron Microscopy (TEM). The Kanazawa gold leaf, known for its ultra-thin foil (100-200 nm thick), is traditionally produced by a method involving paper packing and hammering. In our investigation of gold leaf processing techniques, we noted a critical step: the process requires periodic pauses to unwrap the leaf for cooling when its thickness is reduced to below 1 μ m. This method incorporates periodic cooling pauses, suggesting meticulous temperature control between 100 to 200°C¹, which we infer is crucial for preserving grain characteristics and facilitating plastic deformation without excessive grain growth or structural disruption.

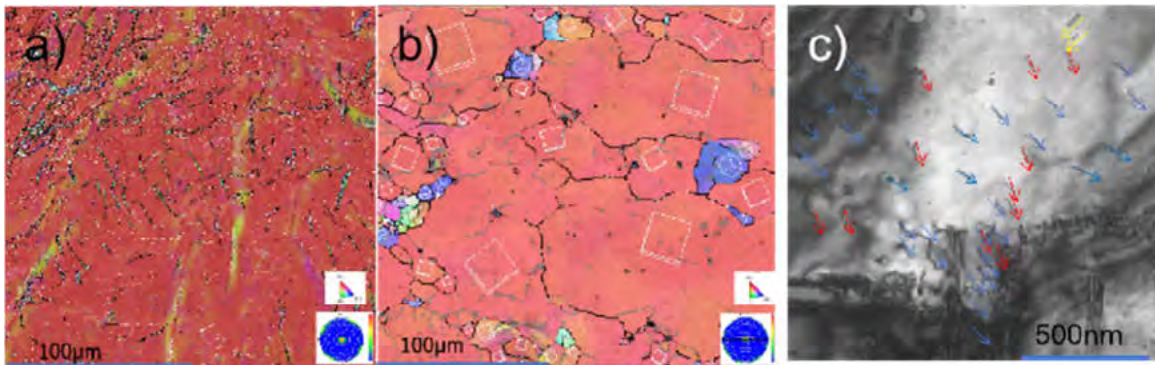


Figure 1a) b) EBSD and anti-polar figure of gold leaf and aluminum leaf (the black line is the grain boundary). c) two beam bright field TEM data of gold leaf, different color of arrows shows different types of dislocations.

In our EBSD analysis, we examined both pure aluminum leaf and gold leaf under identical processing conditions. The analysis revealed a similar $\{001\}$ crystal orientation in both metals. However, a marked difference in grain structure was evident. For aluminum, its lower melting point likely leads to the $\{001\}$ orientation resulting from recrystallization. In contrast, the gold leaf displayed more heterogeneous grains in terms of size and shape. Complementary TEM analysis indicated various types of dislocation activities within the gold leaf, suggesting that the $\{001\}$ orientation is predominantly due to plastic deformation, despite the controlled temperature conditions.

In our detailed analysis of EBSD data for gold leaf we specifically observed a notable reduction in the number of grain boundaries, even leading to their disappearance in certain areas within the $\{001\}$ crystals. Such reduction is possibly due to grain inhomogeneity, cause of a consequence of the low processing temperatures. As this phenomenon the cooler conditions are conducive to increased dislocation activity, essential for the development of specific crystal orientations.

References:

[1] K. Kitagawa, J. MATERIALS SCIENCE 23 (1988) 2810.

First-principles study of the van der Waals ZnO layers

Nadia Maharani Chadiza¹, Hana Pratiwi Kadarisman², Naoya Yamaguchi², and Fumiyuki Ishii²

¹Graduate School of Natural Science and Technology, Kanazawa University, Kakuma-chi, Kanazawa, 920-1192, Japan.

²Nanomaterials Research Institute (NanoMaRi), Kanazawa University, Kakuma-chi, Kanazawa, 920-1192, Japan.

Zinc oxide (ZnO) nanostructures play a pivotal role in advancing electronics, optoelectronics, and sensing devices. The transition from bulk to mono- and bilayer structures has a profound impact on the electronic properties of ZnO [1]. In this study, we investigate how the thickness of these layers influences these properties, which is of paramount importance for nanoscale device applications [2].

To gain insights, we conducted density functional calculations employing the generalized gradient approximation (GGA) with the Perdew-Burke-Ezernhof (PBE) method [3], utilizing the OpenMX code [4]. We calculated the band structures and density of states (DOS) for both monolayer and bilayer ZnO [5]. Additionally, we calculated electronic properties and generated charge density plots to assess changes in electron distribution.

Our band structure analysis revealed a direct band gap in both forms of ZnO. Notably, the transition from a monolayer to a bilayer resulted in a reduction of the band gap from 2.25 eV to 2.19 eV. We will also present on spin splitting, which is important as a material for spintronic devices, and the electric dipole moment that induces it.

Keywords: ZnO, Monolayer, Bilayer, Band Gap, Density Functional Theory

References:

[1] Smith, J. et al., *Nano Lett.*, **18**, 1234(2018).

[2] Jones, R., & Liu, X., *Adv. Mater.*, **32** 1902765(2020).

[3] Perdew, J. P., Burke, K., and Ernzerhof, M., *Phys. Rev. Lett.*, **77**, 3865 (1996).

[4] OpenMX, Open-source package for Material eXplorer, T. Ozaki et al, <http://www.openmx-square.org/>

[5] Doe, J., & White, R., *J. Comput. Chem.*, **42**, 754(2021).

Density functional study of VO₂ growth on hexagonal boron nitride & graphene

Wakil HASAN¹, Mitsuharu UEMOTO¹, Tomoya ONO¹

¹ Department of Electrical and Electronic Engineering, Graduate School of Engineering, Kobe University, 1-1 Rokkodai-cho, Nada-ku, Kobe 651-8501, Japan,

Abstract: Vanadium-dioxide (VO₂) a transition-metal oxide exhibits the insulator-metal transition(IMT) and metal-insulator transition(MIT) following a resistance change of noticeable magnitude[1-2]. These IMT or MIT behaviors can be exploited in different applications such as Mott transistors[3], bolometers[4], smart windows[5], and so on.

The VO₂ as an effective electrical switching device was investigated using the Joule heating effect while focusing on the metallic domain in the VO₂ channel area[6]. In the metallic domain, the effectiveness of the Joule heating devices can be investigated by focusing on VO₂ thin film grown on hexagonal boron nitride(h-BN). 2D h-BN can be a good option for the growth of VO₂ which was investigated experimentally[6-7]. In this study, we choose a theoretical approach to that experimental work. The growth of VO₂ on 2D h-BN and graphene is investigated using the first-principles theoretical method based on density functional theory (DFT). Vienna Ab initio Simulation Package (VASP)[8] is employed to optimize the interface atomic structure of VO₂/h-BN and VO₂/graphene. We use hydrogen atoms with dangling bonds to eliminate the continuity and the 2D materials are put on the top of the VO₂ with inter-layer distance 2Å. The optimized structural model is shown in **Figure 1**. We observe the interaction between the 2D materials and VO₂. The binding energy was also calculated with the growth of VO₂ on h-BN and graphene.

References:

- [1] F. J. Morin, Phys. Rev. Lett. **3**, 34 (1959).
- [2] C. N. Berglund and H. J. Guggenheim, Phys. Rev. **185**, 1022 (1969).
- [3] S. Sengupta *et al.*, Applied Physics Letters **99**, 062114 (2011).
- [4] C. Chen *et al.*, Sensors and Actuators A: Physical **90**, 212 (2001).
- [5] Z. Huang *et al.*, Appl. Phys. Lett. **101**, 191905 (2012).
- [6] S. Genchi *et al.*, Jpn. J. Appl. Phys. **62**, SG1008 (2023).
- [7] S. Genchi *et al.*, Sci Rep **9**, 2857 (2019).
- [8] G. Kresse and D. Joubert, Phys. Rev. B **59**, 1758 (1999).

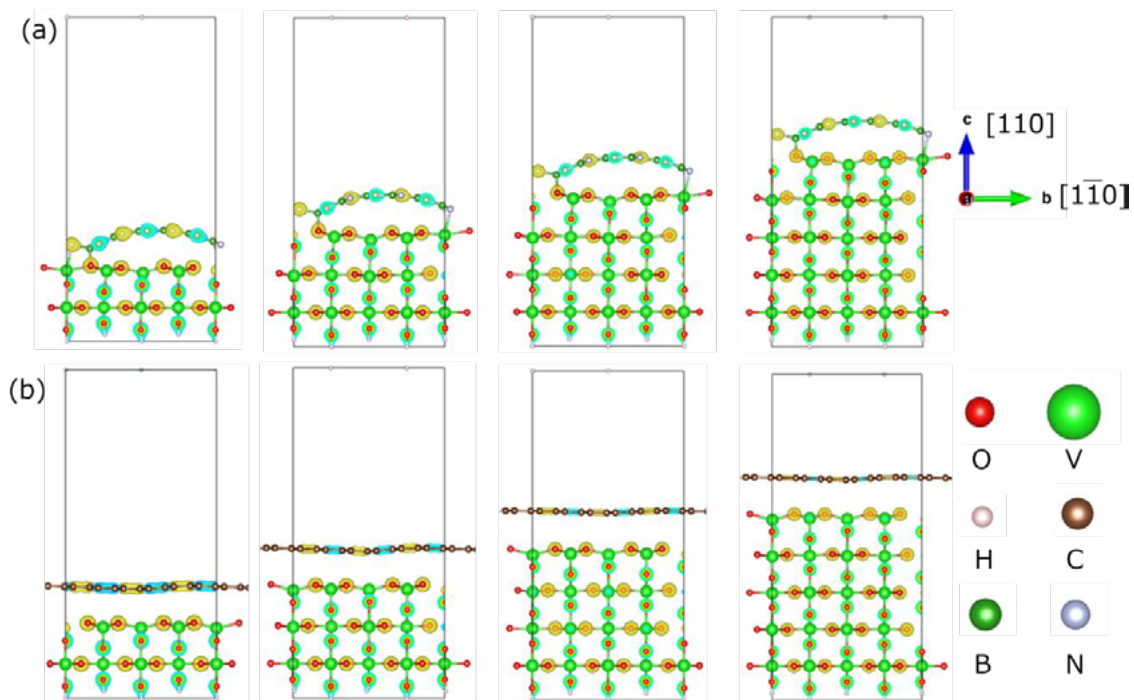


Figure 1: Optimized electron density profile of VO₂ growth on (a) h-BN and (b) graphene.

Phase Conversion to the Air-stable 1T'-MoS₂ by a Chemical Procedure

Keigo Matsuyama¹, Daisuke Kiriya¹

¹ The Univ. of Tokyo, Japan.

Transition metal dichalcogenides (TMDCs), a two-dimensional semiconductor, have recently attracted attention in terms of emerging phenomena and applications based on topological properties [1]. The phase transition from a semiconductive 1H to a metallic 1T phase is not usually preferable and requires surpassing a large energy barrier (~ 0.5 eV/atom) [2]. The 1T phase is thermodynamically unstable, so it changes to a metastable topological 1T' phase by relaxing with lattice distortion. Since the 1T' phase is still in a metastable state, and the conversion to the 1T phase is not preferential, it is difficult to systematically generate the 1T' phase. In this study, we report our results of generating the 1T' phase by a conversion from the semiconducting 1H (2H)-MoS₂. The method is scalable because of a chemical procedure, in addition, we realized the generated state is air-stable.

Figures 1a and 1b show the Raman spectra of mono- and bilayer MoS₂ before and after the treatment with the chemical (molecule-based) treatment. In the treated samples, clear spectral changes were observed, for example, the E' and A' signals were diminished. In addition, the three peaks (J1, J2, and J3) were observed in the region from 150 cm⁻¹ to 333 cm⁻¹; these peaks suggest the phase conversion to the 1T' phase from the original 1H phase. In the presentation, we will discuss the details of the process, the mechanism of the phase conversion, and electrical transport.

References:

[1] X. Qian et al., Science, 346, 1344–1347 (2014).

[2] H. Zhuang et al., Phys. Rev. B, 96, 165305 (2017).

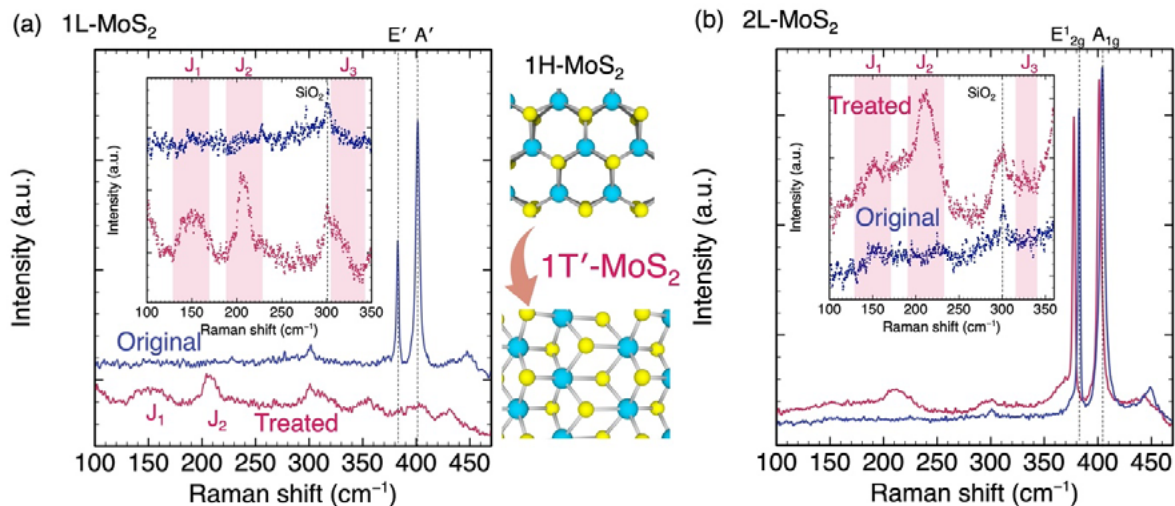


Figure 1. Raman spectra for (a) monolayer and (b) bilayer MoS₂ with the chemical procedure.

Atomic Study of MBE-grown Mn Thin Films on Insulating Substrates

A. Moriyama¹, N. A. Purba¹, K. Shimamura², Y. Obata¹ and Y. Yoshida¹

¹ Dept. of Phys. Kanazawa Univ., 920-1192, Kanazawa, Japan.

² Eng. and Tech. Dept., Kanazawa Univ., 920-1192, Kanazawa, Japan.

α -Mn is one of the single crystals that has the most complicated atomic structure with 58 atoms per unit cell [1] and it has been reported that the Neel temperature, T_N , increases from 95 K to 120 K on glass substrates [2]. In our previous research, we grew α -Mn thin films on the MgO or sapphire substrates by using molecular beam epitaxy (MBE) and performed X-ray structure analysis and low-temperature transport measurements. We clarified that T_N increases regardless of the substrate used and the growth direction [3]. In addition, we observed a resistivity upturn for all samples though the upturn depends on the substrate used in the low-temperature region below 10 K. The upturn is most likely due to the Anderson localization arising from the randomness of interface buffer layers. To confirm the existence of such buffer layers, we investigated the film-substrate interface structure of the α -Mn thin films using a high-angle annular dark-field scanning transmission electron microscope (HAADF-STEM). Cross-sectional HAADF-STEM observation reveals that the size and the structure of the buffer layer are quite different depending on the substrates and explains the relationship between randomness at the interfaces and resistivity upturn. Combining with a detailed thin film X-ray analysis, we determined the interfacial structures and growth models. The details of our experimental results will be reported in the presentation.

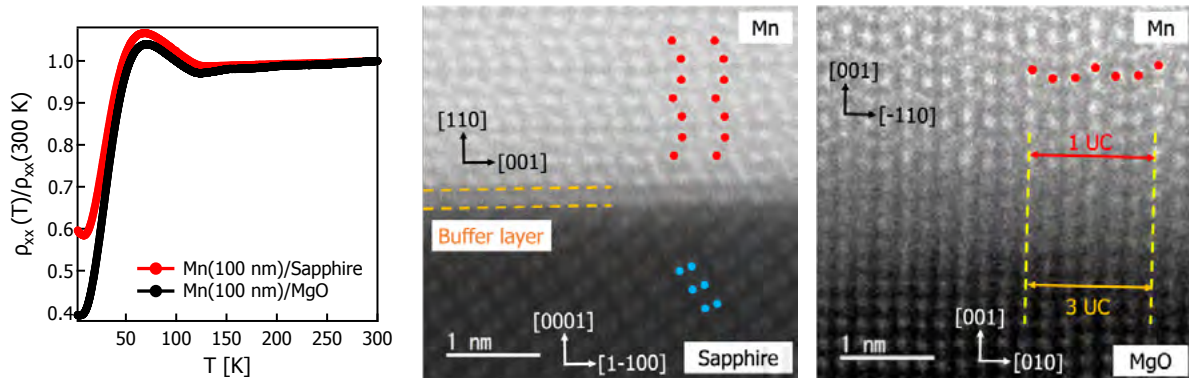


Fig. 1. (Left) Temperature dependence of the resistivity of α -Mn thin films grown on the insulating substrates. Cross-sectional TEM images of (Center) Mn/MgO thin film and (Right) Mn/Sapphire thin film.

References:

- [1] J. S. Kasper and B. W. Roberts, Phys. Rev. **101**, 537 (1956)
- [2] F. Boakye and K. G. Adanu, Thin Solid Films. **279**, 29 (1996)
- [3] A. Moriyama *et al.*, JPS Conf. Proc. **38**, 001073 (2023)

A first-principles study of hydrogen and oxygen adsorption in mercury iodide HgI₂ monolayer

Sulthan W. A. Wisesa¹, Rifky Syariati², Naoya Yamaguchi², Fumiyuki Ishii²

¹ Graduate School of Natural Science and Technology, Kanazawa University, Kanazawa 920-1192, Japan.

² Nanomaterials Research Institute (NanoMaRi), Kanazawa University, Kanazawa, 920-1192, Japan.

Due to the unique properties of 2D materials, such as flexible tuning, no dangling bonds, high mobility, and many more, 2D material photodetectors have become a research interest [1]. A recent theoretical study on mercury-based halide suggested that the material exhibits robust transport and optical properties [2]. Studies have also shown mercury iodide HgI₂ could be utilized as a photoconductor, photodetector, and photocatalyst due to its optical properties [3-5]. The adsorption of hydrogen and oxygen has been shown to alter the structural and electronic properties of materials which could lead to changes in the thermoelectric and optoelectronic properties resulting in a new property of the materials [6-8]. In this study, we investigate the effect of hydrogen and oxygen adsorption on the structural and optoelectronic properties of HgI₂ monolayer by performing the density functional theory (DFT) calculation using the OpenMX code [9].

References:

- [1] K. Zhang, L. Zhang, L. Han, L. Wang, Z. Chen, H. Xing, and X. Chen, *Nano Express*, **2**, 12001 (2021).
- [2] S.S. Sahoo, V.K. Sharma, M.K. Gupta, R. Mittal, and V. Kanchana, *Mater. Today Commun.*, **32**, 102824 (2022).
- [3] Z. P. Zhang, Z. J. Zhang, W. Zheng, K. Wang, H. J. Chen, S. Z. Deng, F. Huang, J. Chen, *Adv. Mater. Technol.*, **5**, 1901108 (2020).
- [4] S.S. Shaker, S.I. Younis, J.M. Moosa, and R.A. Ismail, *Mater. Sci. Semicond. Process*, **135**, 106106 (2021).
- [5] K. Xu, H. Qin, J. Chen, X. Cai, P. Kong, L. Liu, B. Sun, and Y. Chen, *Comput. Mater. Sci.*, **219**, 112007 (2023).
- [6] H. Xu, W. Fan, A.L. Rosa, R.Q. Zhang, and Th. Frauenheim, *Phys. Rev. B*, **79**, 73402 (2009).
- [7] Z. Yang, Y. Zhang, M. Guo, and J. Yun, *Comput. Mater. Sci.*, **160**, 197–206 (2019).
- [8] M. Rassekh, J. He, S. Farjami Shayesteh, and J.J. Palacios, *Comput. Mater. Sci.* **183**, 109820 (2020).
- [9] OpenMX, Open-source package for Material eXplorer, T. Ozaki et al, <http://www.openmx-square.org/>

Figures and figure captions

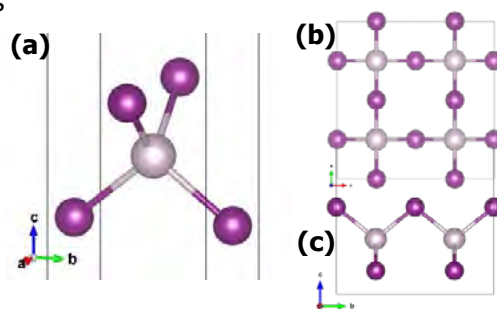


Figure 1: The structure of monolayer HgI₂, (a) unit cell, (b) top view, and (c) side view.

Repeatable growth of segregated germanene by oxidation and reheating

Seiya Suzuki¹

¹ Advanced Science Research Center (ASRC), Japan Atomic Energy Agency (JAEA), Japan.

Germanene is a two-dimensional (2D) sheet of germanium (Ge) with a honeycomb lattice. Recent theoretical studies have predicted several interesting electronic properties of germanene, such as its 2D topological insulators [1]. However, unlike graphene, germanene is easily oxidized in air, making it difficult to realize electrical devices using germanene [2]. To overcome the drawback of the chemical stability of germanene, it is necessary to understand how germanene is oxidized. We therefore began to study the oxidation of germanene and discovered an interesting phenomenon: oxidized germanene can be restored to good quality germanene simply by heating it in an ultra-high vacuum (UHV). Figure 1(a) schematically illustrates the effect of oxidation and reheating of germanene in UHV. Figure 1(b) shows Ge3d X-ray photoelectron spectroscopy (XPS) spectra of germanene (black), oxidized germanene (blue), and reheated germanene. Oxidation was performed by introducing O₂ into the UHV chamber at RT. The XPS spectra clearly show that the oxidized germanene was restored simply by heating in UHV. Figure 1(c) shows the low energy electron diffraction (LEED) patterns of as-grown and oxidized germanene after heating at RT, 250 °C, and 500 °C in UHV. The LEED patterns indicate that the oxidized germanene is fully recovered after heating at 500 °C. The detailed mechanism of the recovery will be discussed in the presentation.

Acknowledgement: The synchrotron radiation experiments (XPS) were performed at the BL23SU of SPring-8 with Proposal No. 2022A3801 and 2023A3801. This work was partially supported by JST, PRESTO Grant Number JPMJPR21B7, Japan.

References:

- [1] M. Ezawa, J. Phys. Soc. Jpn. **84**, 121003 (2015).
 [2] S. Suzuki *et. al.*, Adv. Funct. Mater. **31**, 2007038 (2021).

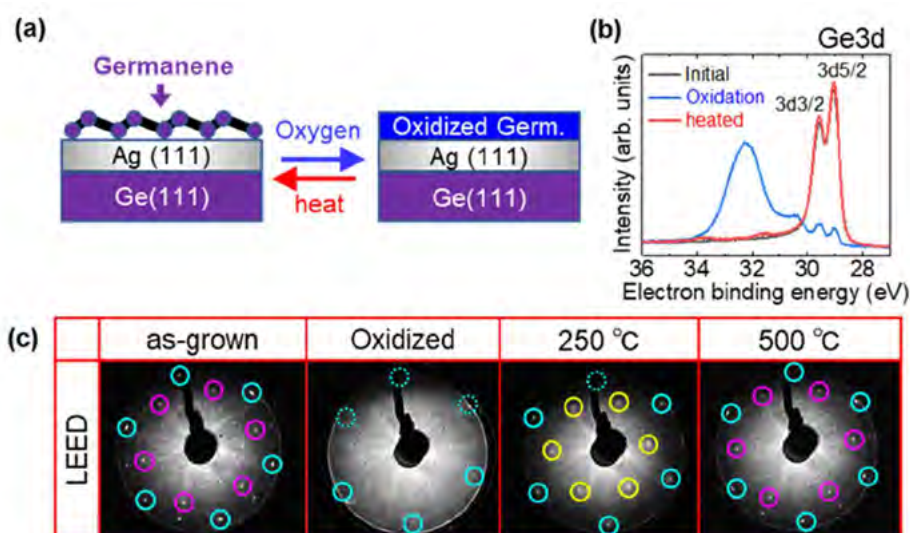


Figure 1. (a) Schematic illustration of the effects of UHV heating on oxidized germanene. (b) XPS Ge3d spectra of germanene as-grown (black), after exposed to O₂ (blue), and after oxidized and reheated (red). (c) LEED patterns of as-grown and oxidized germanene after heated at RT, 250 °C, and 500 °C in UHV. The LEED patterns of germanene indicated that the oxidized germanene was completely recovered after heating at 500 °C.

Research on Ultrathin Sn Films Grown on InSb(111)A for the Growth of Stanene

Takato Yokoo, Yuki Nishita, Antoine Fleurence, Yukiko Yamada-Takamura
School of Materials Science, Japan Advanced Institute of Science and Technology (JAIST),
1-1 Asahidai, Nomi, Ishikawa 923-1292, Japan.

Stanene is a two-dimensional (2D) material made only of tin (Sn). The free-standing form is expected to be a buckled honeycomb structure that is equivalent to α -phase Sn(111) bilayer^[1]. Free-standing stanene is expected to have a larger spin-orbit band gap compared to similar 2D materials made of lighter elements of the group IV ^{[2],[3]}. The experimental realization of a free-standing-like form of stanene would be promising for observing quantum spin hall effect at room temperature^[1]. Recently, experimental realizations of stanene has been reported, but the electronic structure expected for free-standing stanene has not been observed^[4]. One of the reasons could be the lattice mismatch between stanene and the single-crystalline substrates. In this study, we used In-polar indium antimonide wafer, InSb(111)A, as a substrate for the growth of stanene, since the in-plane lattice constant of InSb(111) (4.58 Å) is very close to that expected for free-standing stanene^[5].

The sample preparation and analysis were done in a ultra-high vacuum scanning tunneling microscopy (STM) system. InSb(111)A substrates were cleaned by repeated Ar⁺ ion sputtering and annealing at 460°C. Ultrathin Sn films were grown at room temperature on InSb(111)A substrates. Effect of post-deposition annealing on the sample surface structure using direct current heating were observed *in situ* by low energy electron diffraction (LEED). STM was used to resolve the atomic structure of ultrathin Sn films formed by Sn deposition and post-deposition annealing.

As a function of post-deposition annealing temperature, annealing duration and Sn coverage, a variety of ultrathin Sn layer structures were observed. Among them, a domain structure was found, which has a honeycomb atomic structure inside the domain. The lattice constant of this honeycomb structure was very close to the value calculated for free-standing stanene. The optimization of the size of the region of the domain structure can be achieved by adjusting the duration of the post-deposition annealing. These observation suggest that controlling the growth condition of Sn is important to give rise to stanene on InSb(111)A.

References:

- [1] Y. Xu *et al.*, *Phys. Rev. Lett.* **111**, 136804 (2013).
- [2] S. Balendharan *et al.*, *Small* **11**, 640 (2015).
- [3] C. C. Lee *et al.*, *Phys. Rev. B* **84**, 195430 (2011)
- [4] F. F. Zhu *et al.*, *Nature Mater.* **14**, 1020 (2015).
- [5] T. Osaka *et al.*, *Phys. Rev. B* **50**, 7567 (1994).

Influence of InAs thickness on surface morphology in low-temperature grown MnAs/InAs/MnAs double heterostructure on GaAs (111)B

Md Tauhidul ISLAM*, Masashi AKABORI

School of Materials Science (SMS) and Center for Nano Materials and Technology (CNMT),
Japan Advanced Institute of Science and Technology (JAIST), Japan

The hybrid structures of ferromagnetic and semiconductor have drawn attention because of their possible application in spin field effect transistors (spin-FETs). Using ferromagnetic MnAs and semiconducting thick InAs layers grown on GaAs(111)B by molecular beam epitaxy (MBE), we have created such hybrid structures [1] that have demonstrated some encouraging outcomes in the case of in-plane device applications [2–3]. However, the lithography process limits the ability to reduce channel length for in-plane devices. Therefore, ferromagnetic (FM)/semiconductor (SC)/ferromagnetic (FM) vertical double heterostructures have been prepared by us to circumvent this limitation. The length of semiconductor (InAs) channel can be more easily regulated during the growth process. Growth of InAs at low temperature (LT) is necessary to match the usual growth temperature of MnAs (200-300 °C), although the usual growth temperature of InAs in MBE is ~ 480 °C [4]. One major concern of growing InAs at low temperature is the shorter migration of In adatoms, causing coalescence of them and resulting in 3-D epitaxial growth instead of layer by layer. This may introduce defects on the InAs /MnAs interface and affect the surface quality, crystallinity and magnetic property of top MnAs layer. Thus, we observed the surface morphology of the double heterostructure with varied InAs thickness.

The layers were grown by MBE at As/In beam equivalent pressure (BEP) ratio of ~ 10 for InAs and As/Mn BEP ratio of ~ 250 for MnAs, with a thickness of ~ 180 nm for bottom MnAs, ~ 500 to 100 nm for InAs, and ~ 90 nm for top MnAs. The substrate temperature was fixed to 250 °C. We confirmed the stacking of the tri-layers by cross-sectional scanning electron microscopy (SEM) and energy-dispersive x-ray spectroscopy (EDS) observations. From atomic force microscopic (AFM) images, we observed the nucleation of InAs and MnAs as triangular terraces (Figure 1 (a) and (b) respectively), probably representing the atomic arrangement of (111) plane of GaAs substrate. Surface roughness of LT-InAs increased with increasing thickness (~ 0.7 nm and ~ 5.5 nm for 100 nm and 500 nm LT-InAs single layers respectively). Consequently, with the increase of InAs layer thickness in the double heterostructure, the surface roughness was found to be ~ 2.5 to 4.3 nm (Figure 1(c)), which was not such a severe change. Roughness of top MnAs layer was influenced by the higher roughness of the underneath LT-InAs layer, as we measured the roughness of MnAs single layer on GaAs (111) to be ~ 1.5 nm. The coercivity of the top MnAs layer is presumably higher due to its lower thickness and higher roughness than the bottom MnAs layer. Therefore, we performed in-plane magnetization measurement at 4 K by superconducting quantum interference device (SQUID) magnetometer (Figure 1 (d)) and got the evidence of different magnetic switching behavior (difference in coercivity).

References:

- [1] Md E. Islam, M. Akabori, J. Crystal Growth 463, 86 (2017).
- [2] Md E. Islam, M. Akabori, Physica B 532, 96 (2018).
- [3] Md E. Islam et al., AIP Advances 9, 115215 (2019).
- [4] M. Yano et al., Jpn. J. Appl. Phys. 16, 2131 (1977).

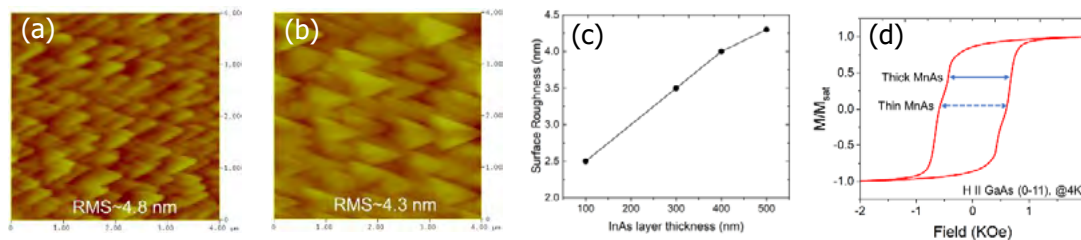


Figure 1: AFM image of (a) InAs(500nm)/MnAs, (b) MnAs/InAs(500nm)/MnAs; (c) InAs thickness vs surface roughness; (d) Magnetization measurement of the double heterostructure.

Wet etching of AlGa_N via removal of altered layer obtained by Ti-AlGa_N reaction

Japan Advanced Institute of Science and Technology

G. Jieensi¹, Y. Deng², J. Choi³, and T. Suzuki⁴

E-mail: ¹s2210409@jaist.ac.jp, ²yuchen94@jaist.ac.jp, ³s2310101@jaist.ac.jp, ⁴tosikazu@jaist.ac.jp

Towards normally-off operations of GaN-based field-effect transistors (FETs), gate recess structures are widely employed [1]. In order to obtain a recessed structure, two types of etching method, wet etching and dry etching can be utilized. Wet etching removes semiconductors through chemical reactions, leading to less lattice damage and interface contamination, which is favorable for many device fabrication processes. However, since GaN-based semiconductors are chemically quite stable, additional treatments are usually demanded, such as ultraviolet illumination for photoelectrochemical etching, making the process more complicated [2]. Thus, for gate recessed AlGa_N/GaN FETs, dry etching is mainly used owing to advantages of simple process, high etching efficiency, and suitability for fine-structure fabrication. However, lattice damages and interface contaminations are inevitably caused by dry etching [3], leading to deteriorations of device performances, such as a reduction in electron mobility [4] and an increase in low-frequency noise [5]. Recently, for Ti-based Ohmic contacts to GaN, it was found that there is an nm-order altered layer in GaN caused by a Ti-GaN reaction, and the altered layer can be removed by wet etching with a high quality remaining surface [6]. Therefore, by removing an altered layer obtained by a Ti-AlGa_N reaction, we can expect wet etching of nm-order AlGa_N. Moreover, by repeating the cycle of the nm-order AlGa_N etching, precise etching depth control can be expected. In this study, we investigated the possibility of this etching method.

Figure 1 shows etching method in this study. As one cycle, a thin Ti layer is deposited and annealed for 5 min at 575°C on an AlGa_N/GaN heterostructure, followed by wet etching of the Ti layer and the altered layer by HF. This cycle is repeated for several times. Figure 2 shows the atomic force microscope (AFM) image and the cross-sectional profile for the surface after five-cycle etching. The root mean square (RMS) roughness after the etching is ~ 0.5 nm, while that before the etching is ~ 0.3 nm, showing that a relatively smooth surface is obtained by this etching method. From the cross-sectional profile, we find an etching depth $d \simeq 5$ nm. Figure 3 shows the etching depth and the etched surface RMS roughness as functions of the etching cycle number, from which we find that the one-cycle leads to $\simeq 1$ nm etching.

In summary, we investigated AlGa_N etching via removal of a nm-order altered layer obtained by a Ti-AlGa_N reaction. By repeating the cycle of the nm-order AlGa_N etching, we can obtain precisely controlled etched depths and relatively smooth etched surfaces. This etching method can be applied to gate recess of AlGa_N/GaN FETs.

References

- [1] F. Roccaforte, G. Greco, P. Fiorenza, and F. Iucolano, *Materials* **12** (2019).
- [2] D. Zhuang and J. Edgar, *Mater. Sci. Eng. R* **48**, 1 (2005).
- [3] S. Pearton and R. J. Shul, *MRS Internet J. Nitride Semicond. Res.* **5**, 11 (2000).
- [4] D. D. Nguyen, T. Isoda, Y. Deng, and T. Suzuki, *J. Appl. Phys.* **130**, 014503 (2021).
- [5] D. D. Nguyen, Y. Deng, and T. Suzuki, *Semicond. Sci. Technol.* **38**, 095010 (2023).
- [6] K. Uryu, Y. Deng, S. P. Le, and T. Suzuki, *AIP Adv.* **13**, 075002 (2023).

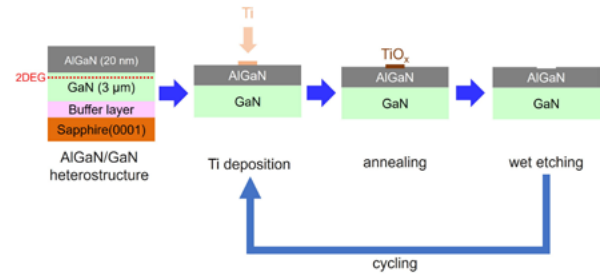


Figure 1: The etching method. As one cycle, a nm-order AlGa_N is etched via removal of an altered layer obtained by Ti-AlGa_N reaction. This cycle is repeated.

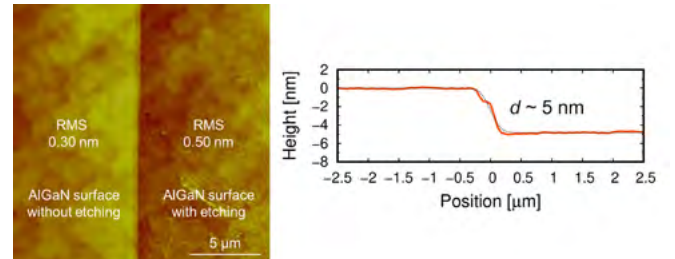


Figure 2: The AFM image and the cross-sectional profile after five-cycle etching.

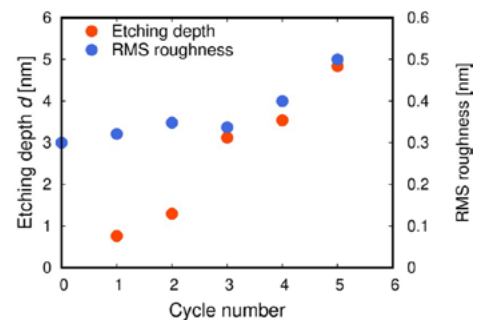


Figure 3: The etching depth and the etched surface RMS roughness as functions of the etching cycle number.

MnSb and InSb grown on GaAs (111)B for spin-FET application

Md. Faysal Kabir^{1*}, Md Tauhidul Islam¹, Masashi Akabori¹

¹Center for Nano Materials and Technology (CNMT), Japan Advanced Institute of Science and Technology (JAIST)

1-1 Asahidai, Nomi, Ishikawa 923-1292, Japan

Ferromagnetic metal/semiconductor (FM/SC) hybrid structures are poised to lead in a new era in the fabrication of spintronic devices, particularly in the development of spin field-effect transistors (spin-FETs) [1]. Hexagonal MnSb, a ferromagnetic metal, demonstrates consistency with III-V compounds like GaAs and InSb [2,3]. InSb, a narrow-gap semiconductor, exhibits strong spin-orbit coupling. Consequently, the MnSb/InSb hybrid structure emerges as an appealing FM/SC configuration for spin-FET application. Furthermore, the (111)B surfaces of III-V compounds are attractive due to their crystallographic compatibility with hexagonal MnSb and cubic InSb structures [3,4]. In our previous research, through scanning electron microscopy (SEM), energy-dispersive X-ray spectroscopy (EDS), Atomic force microscope (AFM), X-ray diffraction (XRD), and superconducting quantum interface device (SQUID), we determined that the optimum growth temperature for MnSb/GaAs (111)B was between 400 °C and 500 °C [4]. This study presents our recent findings on MnSb and InSb growth on GaAs (111)B using molecular beam epitaxy (MBE) and their subsequent characterization. We varied the Sb/Mn beam equivalent pressure (BEP) ratio from 1 to 6 at 400 °C. Through SEM and XRD (Figure 1(a)), we identified the optimum BEP to be between 3 and 6. Additionally, we measured magnetization curves using SQUID magnetometer, as depicted in Figure 1(b). Our results indicated favorable properties for the sample with a BEP of Sb/Mn~3. Similarly, for InSb growth on GaAs (111)B, we varied the growth temperature from 400 °C to 500 °C. In XRD, all the samples showed InSb (111) peaks and some additional peaks. The growth sample at 400 °C displayed highly prominent InSb (111) peaks with no discernible peaks from any other materials, as shown in Figure 1 (a). While examining the surface using SEM, we identified dome-like structures on the sample grown at 500 °C and observed a non-uniform surface for the 450 °C sample. Conversely, the surface of the sample grown at 400 °C appeared more uniform and was adequately covered by InSb. Hall measurements with van der Pauw geometry, we obtained a room temperature electron mobility of 5000 cm²/V-s with an electron concentration of 1.6×10¹⁷ cm⁻³ in the sample grown at 400 °C. Subsequently, we evaluated the surface roughness of the satisfactory MnSb and InSb samples employing AFM. Through a comprehensive analysis of growth and characterization, we identified superior MnSb and InSb samples for the prospective InSb/MnSb hybrid structure on the GaAs (111)B substrate. This hybrid structure holds promise as a high-performance spin-FET device, with magnetically improved MnSb serving as source/drain and conductive InSb with spin-orbit coupling acting as the channel.

References:

[1] S. Datta and B. Das, Appl. Phys. Lett. 56, 665 (1990).

[2] H. Akinaga et al., Appl. Phys. Lett. 70, 2472 (1997).

[3] Md. E. Islam and M. Akabori, J. Crystal Growth 463, 86 (2017).

[4] M.F. Kabir, M. T. Islam, S. Komatsu, and M. Akabori, Jpn. J. Appl. Phys. To be published.

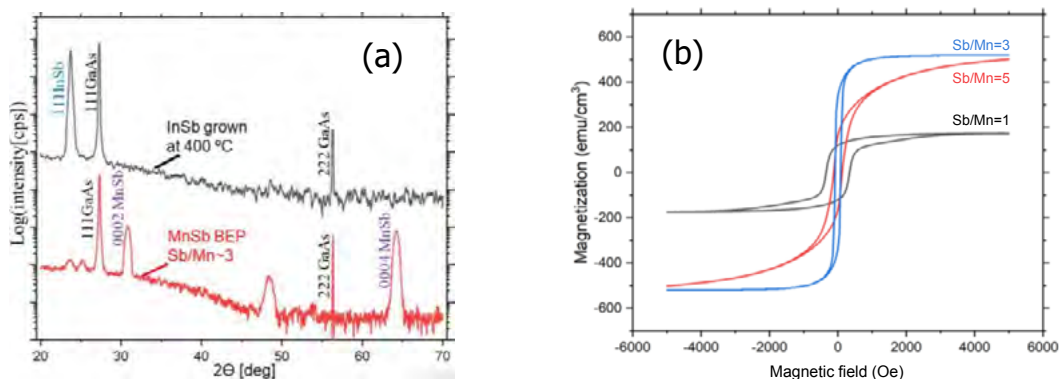


Figure 1: (a) XRD and (b) Magnetization curves of MnSb samples

Synthesis and optical properties of high-quality monolayer Janus MoSSe on hBN substrates

Tomoya Ogawa¹, Wenjin Zhang¹, Hiroshi Nakajo^{2,3,4}, Soma Aoki^{2,3}, Takahiko Endo¹, Yusuke Nakanishi¹,
Kenji Watanabe⁵, Takashi Taniguchi⁶, Toshiaki Kato^{2,3}, Yasumitsu Miyata¹

¹ Department of Physics, Tokyo Metropolitan University, Hachioji, Tokyo, Japan.

² Graduate School of Engineering, Tohoku University, Sendai, Miyagi, Japan.

³ Advanced Institute for Materials Research (AIMR), Tohoku University, Sendai, Miyagi, Japan.

⁴ KOKUSAI ELECTRIC CORP., Toyama, Japan.

⁵ Research Center for Functional Materials, NIMS, Tsukuba, Ibaraki, Japan.

⁶ International Center for Materials Nanoarchitectonics, NIMS, Tsukuba, Ibaraki, Japan.

Janus transition metal dichalcogenides (TMDCs) have attracted much attention due to their asymmetric structure and related physical properties. So far, Janus TMDCs have been synthesized by elemental replacement of the top layer of TMDCs by plasma treatment [1,2]. However, the synthesis of high-quality Janus TMDCs is still a significant challenge. In this study, we have investigated the structure and optical properties of Janus MoSSe monolayers synthesized on hexagonal boron nitride (hBN). MoSe₂ monolayers were grown by CVD on SiO₂/Si and hBN substrates (Fig.1a). The Se atoms on the top layer were replaced by S atoms by H₂ plasma treatment at room temperature using sulfur flakes as a chalcogen source (Fig.1b). PL spectroscopy showed a narrower and blue-shifted PL peak for Janus MoSSe on hBN (Fig.1c). Kelvin Probe Force Microscopy (KPFM) observations revealed that the Janus MoSSe on SiO₂/Si has many cracks (Fig.1d), whereas such cracks were never observed for the Janus MoSSe on hBN (Fig.1e). The crack formation can be understood as the introduction of tensile strain due to the lattice shrinkage associated with the chalcogen substitution. In other words, such tensile strain was suppressed on hBN because of the atomically ultra-flat surface of hBN [3]. These results indicate that the suppression of lattice strain is essential for the preparation of uniform and large grains of Janus TMDC monolayers.

References:

[1] DB. Trivedi et al., *Adv. Mater.* **32**, 2006320 (2020).

[2] Y. Qin et al., *Adv. Mater.* **34**, 2106222 (2022).

[3] Y. Kobayashi et al., *ACS Nano* **9**, 4056 (2015).

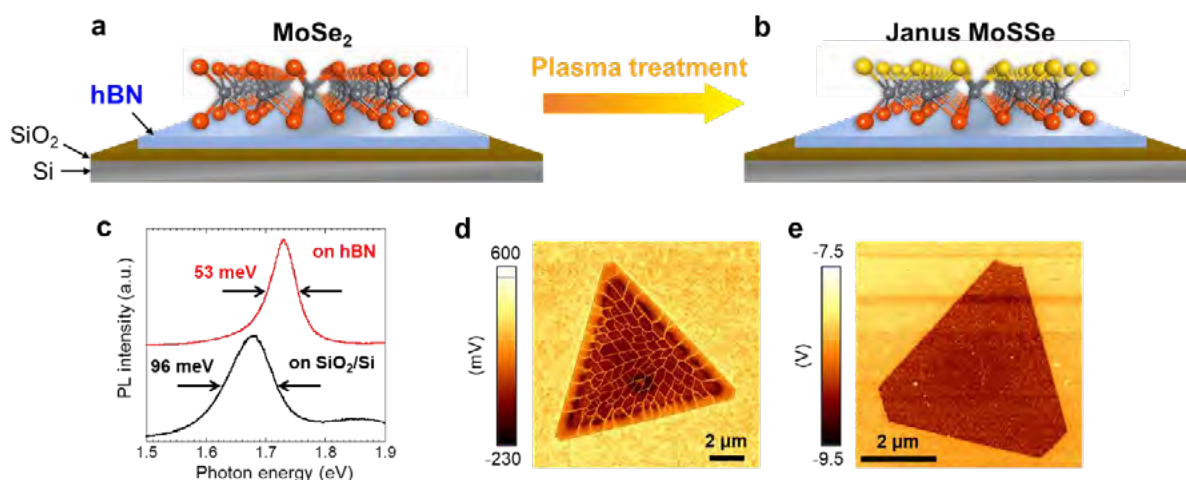


Fig. 1. Structural models of (a) monolayer MoSe₂ and (b) monolayer Janus MoSSe on hBN substrate. (c) PL spectra of Janus MoSSe monolayers on SiO₂/Si and hBN substrates. KPFM images of Janus MoSSe monolayers on (d) SiO₂/Si and (e) hBN substrates.

Focusing Optics to Improve Beam Spot Properties at the XPEEM/LEEM Endstation of the ESM beamline at the NSLS-II

Tatsuki Nagano¹, Abdullah Al-Mahboob² and Jerzy T. Sadowski²

¹ School of Materials Science, Japan Advanced Institute of Science and Technology, 1-1 Asahidai, Nomi Ishikawa, 923-1292, Japan.

² Center for Functional Materials, Brookhaven National Laboratory, Upton, NY 11973, U.S.A.

The x-ray photoemission electron microscopy / low-energy electron microscopy (XPEEM/LEEM) endstation of the Electron Spectro-Microscopy (ESM) beamline of the NSLS-II has both microscopy and spectroscopy modes^[1]. For the spectroscopy modes, the micro-spot ARPES in particular, the spot size of the incident beam is typically much larger than the micrometer-sized selected area apertures (Φ 0.75, 1.5, 5 μ m). This contributes to a rise in the background signal (noise) from the photoelectrons created from beyond the area of interest. The resulting data need to be processed by subtracting the time-averaged background signal. Reducing the spot size, particularly for the energy range of 40-100eV, would significantly shorten the acquisition times and improve the signal/noise ratio in the spectroscopic data.

In this study, our goal was to reduce the spot size by inserting the Fresnel zone plates in the beam path, between the last refocusing mirror and the sample. To design the plates, we need to know the effective optical focal length. We have performed theoretical calculations, considering the light intensity should be a superposition of Gaussian shapes when the light path is precisely at the effective optical focal length. Based on these calculations we fabricated a prototype zone plate using the focused-ion beam (FIB) tool. Preliminary tests revealed that the prototype zone plate can effectively focus the beam, however at higher energies (\sim 100eV) than the intended one (50eV). This indicates that the design needs to be revised to optimize the focal point of the zone plate. Fabrication and testing of the revised optics is currently underway.

This research used resources of the Center for Functional Nanomaterials and the National Synchrotron Light Source II, which are U.S. Department of Energy (DOE) Office of Science facilities at Brookhaven National Laboratory, under Contract No. DE-SC0012704.

References:

[1] <https://www.bnl.gov/cfn/equipment/details.php?q=300164>

Observation saccharides distribution in rice grains by Sum Frequency Generation confocal microscopy

R. Mamiya¹, G. Mizutani¹, H. Noju¹, Y. Wang¹, A. Matsubara¹ and Y. Nakamura²

¹ School of Materials Science, Japan Advanced Institute of Science and Technology, Japan.

² Starch Technologies, Co., Ltd., Akita Prefectural University, Japan.

Rice is a food that almost all Japanese eat every day, but there is still much that is unknown about its structure. New methods are needed to further elucidate the physical properties of this rice.

Our research group used a sum frequency microscope. SFG is only generated from materials that don't have spatial inversion symmetry, and SFG is also allowed for chiral molecule such as a biomolecule. Using this property, SFG microscopy can selectively observe only sugars in rice.

Previously, our group observed rice grains using an SHG microscope[1]. As a result, SH responses were observed in rice embryo and hypocotyl. However, the sugars species has not yet been elucidated. In this study, we aimed to investigate sugars distributed in the embryo by SFG microscopy, which can discriminate different molecular species within a substance. The distribution of substances in the hypocotyl will be discussed by comparing the SFG spectra at the hypocotyl with the spectra of the expected sugars species.

References:

[1] Yue Zhao et al. "Ungerminated Rice Grains Observed by Femtosecond Pulse Laser Second Harmonic Generation Microscopy", *J. Phys. Chem. B* 2018, 122, 7855-7861

[2] Wang Yifei et al. "共焦点和周波顕微鏡による稲種子中の糖鎖の観察", JAIST Thesis, 2022.

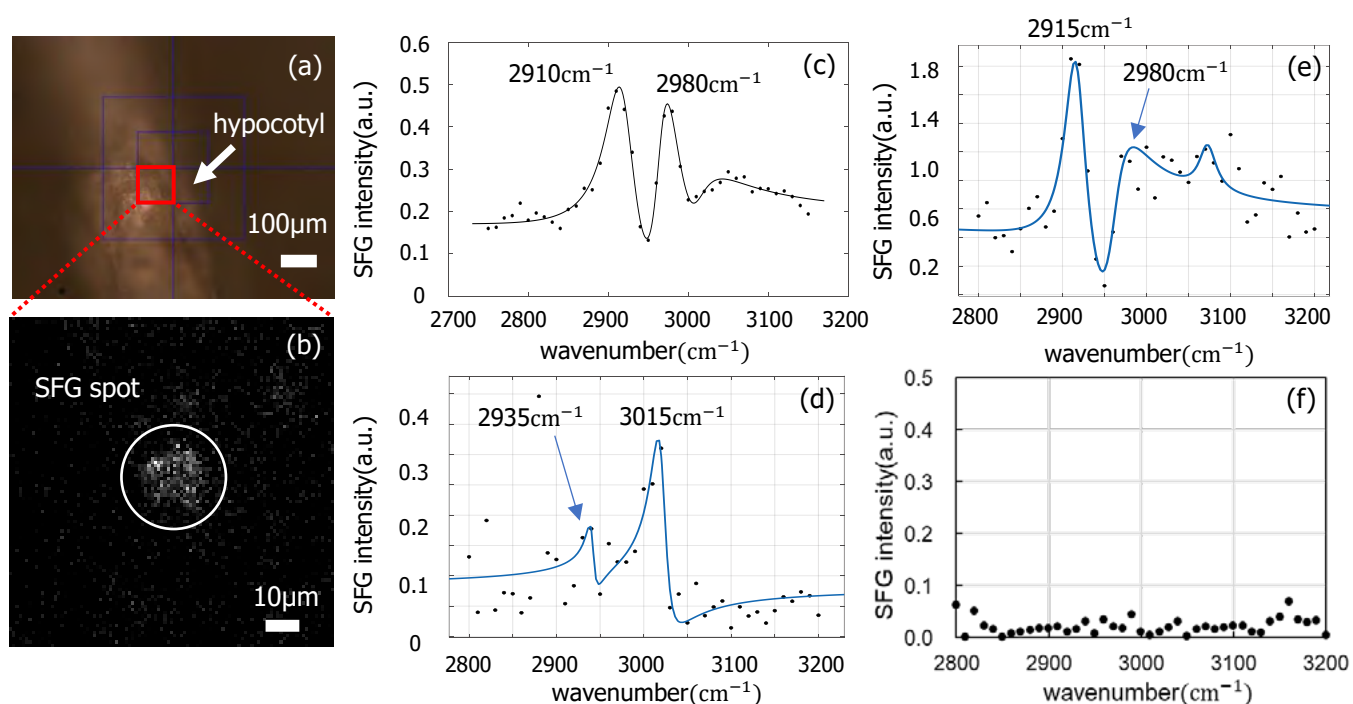


Fig. 1 Ungerminated glutinous rice grain images. (a) Microscopic image of hypocotyl, and (b) SFG image. SFG spectrum with (c) amylopectin reference materials [2], (d) hypocotyl, (e) CCL and (f) embryo.

Observation before and after addition of trivalent metal ions to SACRAN cast films using femtosecond laser SHG microscopy

Kohei Tsujimura¹, Goro Mizutani¹, Phan Dinh Thang¹, Kosuke Okeyoshi¹, Maiko Okajima², Tatsuo Kaneko²

¹Japan, Japan Advanced Institute of Science and Technology.

²China, School of Chemical and Material Engineering, Jiangnan University.

SHG microscopy enables selective observation of inversion symmetry breaking without the need for staining and thermal damage. Sacran, a recently discovered polysaccharide, has received significant attention due to its diverse characteristics. Despite sacran's confirmed metal adsorption capability[1], the detailed mechanism behind this ability remains unclear. This study aims to elucidate the SHG response behavior of sacran when trivalent metal ions are adsorbed onto it, and to contribute to the understanding of such a mechanism.

Figure 2 below shows a slightly higher number of SHG spots than Fig. 1. The SHG intensity observed in Fig. 1(b) (851 a.u.) surpasses that in Figs. 2(b) and 2(e) (208 a.u. and 255 a.u.). The experimental results suggest that the adsorbed metal cations Nd^{3+} or Er^{3+} bind to the sacran anions, reducing the intensity of the local electric field in SHG-active sacran aggregates. On the other hand, Nd^{3+} and Er^{3+} appears to lower the threshold of sacran aggregates for becoming SHG active and increases the number of SHG spots.

[1] M. Okajima, T. Bamba, Y. Kaneso, K. Hirata, S. Kajiyama, E. Fukusaki, and T. Kaneko, "Supergiant ampholytic sugar chains with imbalanced charge ratio form saline ultra absorbent hydrogels," *Macromolecules* 41, 4061–4064 (2008).



Figure 1. Linear, SHG and 2PEF images of the original 0.5 wt% sacran solution (13 spots)

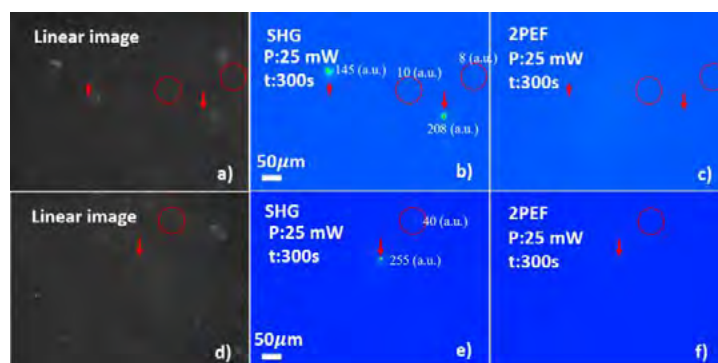


Figure 2. Linear, SHG and 2PEF images of the original sacran solutions absorbed metal ions, (a-c) Er^{3+} (32 spots), (d-f) Nd^{3+} (23 spots)

Development of a of Cryogenic High Magnetic Field Scanning Tunneling Microscope Integrated with Microwave Irradiation Capability

Erlina Tik Man^{1*}, Hiroki Maekawa¹, Takaya Shimokawa¹, Kazutoshi Shimamura², Yasuo Yoshida¹

¹Department of Physics, Kanazawa University, Kanazawa 920-1192, Japan

² Instrumental Analysis Division, Engineering and Technology Department, Kanazawa, Ishikawa 920-1192, Japan

E-mail (presenter): erlina@stu.kanazawa-u.ac.jp

Spin-polarized scanning tunneling microscope (SP-STM) has demonstrated the capability of exploring the magnetic properties of materials at the atomic level for the past few decades. The integration of STM with electron spin resonance (ESR) measurement enhances our ability to detect spin dynamics with a level of sensitivity unattainable by STM alone. Furthermore, STM with microwave irradiation has wider potential such as Shapiro steps and photo-induced tunneling for superconductors. We installed semirigid coaxial cables with a loop antenna to our low-temperature and high-field STM (down to 1.5 K and up to 8 T), enabling us to operate ESR-STM at frequencies up to 40 GHz. We also designed a coplanar waveguide at the STM sample stage to compare and investigate the most suitable design for microwave irradiation on the sample inside the STM head. The presentation will discuss the design and construction of ESR-STM in detail.

Keywords: scanning tunneling microscope, electron spin resonance, low-temperature physics

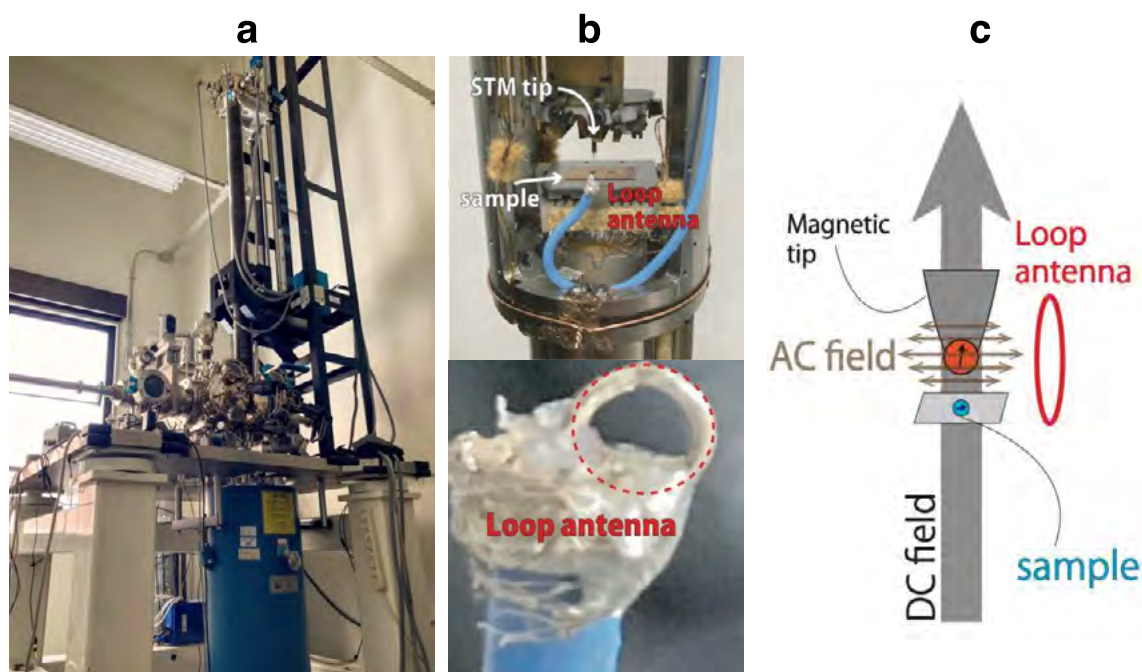


Fig.1 (a) Cryogenic high-magnetic field STM System, (b) Loop antenna for microwave irradiation, and (c) Schematic diagram of ESR-STM measurement

Structural and chemical analysis of tungsten tips for scanning probe microscopy prepared by flame etching

Yohei Nakano¹, Nobuhiko Utsunomiya¹, Toyoko Arai¹, Masahiko Tomitori²

¹Graduate School of Natural Science and Technology, Kanazawa University, 920-1192 Japan

²Japan Advanced Institute of Science and Technology, 923-1292, Japan

Control of the quality of a scanning tip is crucial to determine the performance of scanning probe microscopy (SPM). The tip should be atomically sharp with a stable atomic arrangement and have reproducible physical and chemical properties. Recently, a quick and clean method to prepare the tip of high-temperature-melting metal wires such as tungsten (W) by burning in flame was proposed; named flame etching method [1], as shown in Fig. 1. In comparison to electrochemical etching, chemical residues could be reduced. In the present study, we burned W wires in a high-temperature (~ 2500 °C) flame of a carbon-free hydrogen-oxygen ($H_2:O_2=2:1$) gas burner which sublimated W oxides to make it thin, and characterized them by scanning electron microscopy (SEM), transmission electron microscopy (TEM), and scanning Auger electron microscopy (SAM).

Figure 2 shows the SEM images of the tip of a flame-etched W wire with a diameter of 0.1 mm. The tip surface was surrounded by facets, forming a polyhedral shape, probably due to the difference in oxidation rates of tungsten crystal planes in the flame. Differences in the shape of the tungsten tip were observed, which depended on the flame-etching time. Thus, we developed a setup to control the burning time with a solenoid pinch valve to stop the gas flow at the precision of a few ten milliseconds, and determined the crystal plane index of each facet based on electron diffraction using TEM. We also focused on how to make the tungsten tip clean. From SAM analysis, it was found that the tip surface was covered with oxide layers. To remove the layers, the tip was heated using a blue laser of 450 nm in wavelength and 9 W max. in power in a high vacuum. The details of the shape and chemical analysis of the flame-etched W tip will be discussed.

This work was supported by KAKENHI (21K18191, 22H00279), Japan Society for the Promotion of Science, and partly by Advanced Research Infrastructure for Materials and Nanotechnology in Japan (ARIM) of the Ministry of Education, Culture, Sports, Science and Technology (MEXT) under Grant Number JPMXP122JI0019, JPMXP1223JI0028.

References:

[1] T. Yamaguchi et al., Rev. Sci. Instrum., 2019, **90**, 063701.

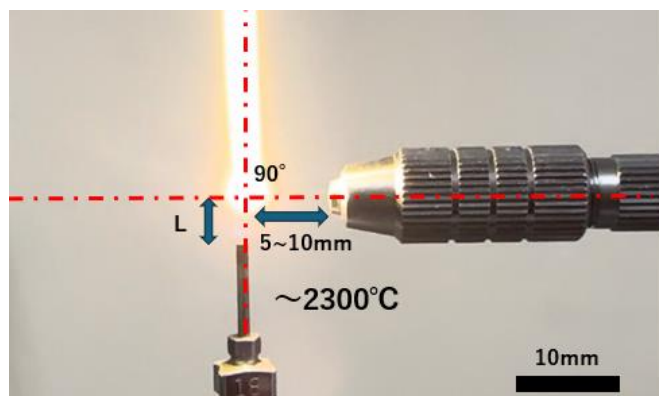


Fig. 1 The fabrication of a tungsten (W) tip by flame etching. The W atoms were sublimated from the W surface as WO_3 which has a higher vapor pressure.

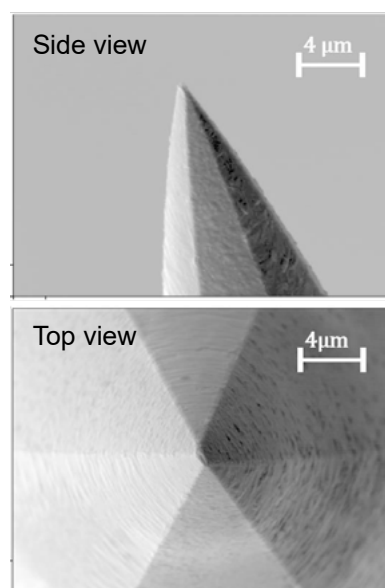


Fig. 2 SEM images of the flame-etched W tip.

Simulation of harmonic generation in silicon nanocylinder

Gosuke Matsuura¹, Koki Kihara¹, Shunsuke Yamada², Mitsuharu Uemoto¹,

¹ Graduate School of Engineering, Kobe University, Japan.

² National Institutes for Quantum Science and Technology (QST), Japan.

Nano-optical devices utilizing all-dielectric nanoparticles and meta-surface for nonlinear optical effects are desired to realize highly efficient optical wavelength conversion and waveform shaping. Computational electromagnetic simulations have been extensively used in this research field to design these nano-optical devices. Besides, a quantum mechanical description of electron dynamics within the materials becomes indispensable under short and intense laser fields. We develop the multiscale method, which combines finite-difference time-domain (FDTD) electromagnetic calculations and first-principles electron dynamics calculations [1-2]. In quantum mechanical calculations, the time-dependent density functional theory (TDDFT) has been used for analyzing laser-matter interactions ("Maxwell+TDDFT") [3]. However, it requires a lot of computational cost. We also develop the semiconductor Bloch equation (SBE)-based multiscale calculation ("Maxwell+SBE"). Owing to SBE's less computational cost than TDDFT, the Maxwell+SBE is capable of large scale device models.

In this study, we utilize the Maxwell+SBE method to simulate light propagation in a silicon nanocylinder array under the high-intensity laser pulses. An enhancement of electric field due to Mie resonance caused by the cylinder and light focusing by lensing effect [See Fig. (a)]. This behavior is significantly differs that observed from the previously studied nanofilm structure [3]. The power spectrum analysis of the electric field indicated the presence of higher-order harmonic components [Fig. (b)]. We analyze the effect of varying the size and spacing of the nanocylinder on the intensity of the electric field. The results shows that there is a dependence on the size of the cylinders, with a maximum around 25 nm in radius, coinciding with Mie resonance condition. We also calculate the frequency-resolved electric field profile of propagating light and investigate the characteristics of profiles representing each harmonic order [See Fig. (c)].

References:

[1] K. Yabana *et al.*, Phys. Rev. B 85, 045134 (2012)

[2] M. Uemoto and K. Yabana., Opt. Exp. **30**, 23664-23677 (2022)

[3] S. Yamada *et al.*, Phys. Rev. B **107**, 035132 (2023)

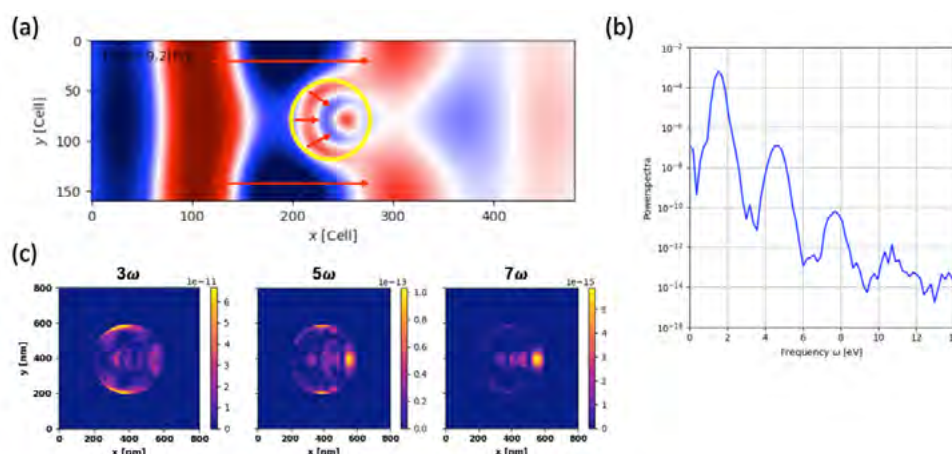


Figure Calculation results: (a) electric field profile. (b) power spectra.

(c) frequency-resolved current density profile

Coherence Properties Improvement of Scanning Diamond Quantum Probes Fabricated by Ga⁺ Focused Ion Beam

Dwi Prananto¹, Yifei Wang¹, Kunitaka Hayashi¹, Toshu An¹

¹ School of Materials Science, Japan Advanced Institute of Science and Technology, Japan

The nitrogen-vacancy (NV) centers-hosting diamonds have been considered versatile quantum sensors to study broad condensed matter physics phenomena, ranging from thermal, and electrical, to magnetic phenomena [1]. Combined with atomic force microscopy, diamond NV probes offer high sensitivity and high resolution at the nanoscale [2], enabled by its atomic-scale quantum spin sensor and its proximity to the measurement target. We developed a simple method to fabricate diamond NV probes crafted by laser cutting and Ga⁺ ion FIB milling [3] and a post-fabrication treatment to retain its quantum spin coherence properties. Prior to the FIB fabrication, the diamond-hosted NV centers layer (40 nm beneath the surface) is coated by polyvinyl alcohol and subsequently by Pt-Pd to minimize possible detrimental effects caused by Ga⁺ ions bombardment during the fabrication process. Post-fabrication UV/ozone exposure to the probe improves its surface condition by oxygen-termination, stabilizing the NV centers' charge state and diminishing noise-inducing surface radicals [4]. The effectiveness of this post-fabrication treatment is indicated by the improvement of the probe's coherence properties including Rabi oscillation (two-level spin state oscillation) contrast improvement by nearly 2 times, the spin-coherence Hahn echo T₂ by 10 times, and longitudinal spin relaxation T₁ by nearly 2 times. To demonstrate the ability of the diamond NV probe as a scanning quantum probe, we image the magnetic domain structure of a ferrimagnetic garnet (BiLu)₃Fe₅O₁₂, showing the ability to resolve a few hundred-nanometer magnetic domain wall structures.

References:

[1] F. Casola, T. van der Sar, A. Yacoby, Nat. Rev. Phys. 3, 17088 (2018).

[2] P. Maletinsky et al., Nat. Nanotechnol. 7 [5], 320 (2012).

[3] Y. Kainuma et al., J. Appl. Phys. 130 [24], 243903 (2021).

[4] H. Yamano et al., Jpn. J. Appl. Phys. 56 [4S], 04CK08 (2017).

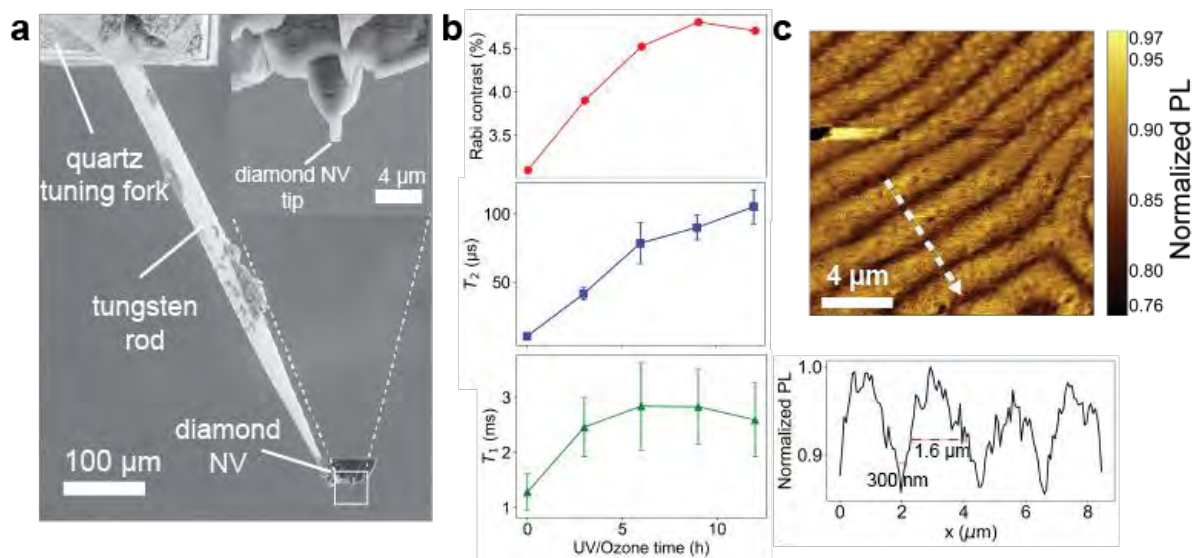


Fig. 1. **a.** SEM image of the FIB fabricated diamond NV probe. **b.** Coherence properties of the diamond NV probe; Rabi oscillation contrast (upper panel), T₂ Hahn echo (middle panel), T₁ (bottom panel) as a function of UV/ozone exposure time. **c.** Image of the magnetic domain structure of (BiLu)₃Fe₅O₁₂ obtained by acquiring photoluminescence (PL) from the diamond NV probe while scanning over an area over the surface of the ferrimagnetic sample (upper panel). The bottom panel is the line-cut (dashed line in the upper panel) of the PL image.

Stray field imaging via diamond NV center probes fabricated by using Focused Ion Beam

¹Wang Yifei, Dwi Prananto, Kunitaka Hayashi, Toshi An

¹School of Materials Science, Japan Advanced Institute of Science and Technology

Email: s2220010@jaist.ac.jp

NV (Nitrogen-Vacancy) center in diamond is a defect structure where one carbon is substituted by one nitrogen atom with a neighboring carbon vacancy. The spin states in the negatively charged NV center can be excited by a laser to generate fluorescence and their magnetic resonances split by the external magnetic field are detected via the ODMR (Optically Detected Magnetic Resonance). Therefore, NV center can be used as a probe to measure stray magnetic fields from magnetic materials. We fabricated a scanning NV center probe for imaging the magnetic samples by using FIB (Focused Ion Beam) [1].

For the probe making process, first, nitrogen ions were implanted into the diamond and annealed at 900 °C for about 2 hours to create NV centers. Second, about 160 nm Pt-Pd film was deposited on the diamond to protect the NV centers, and the diamond was fabricated by using FIB to create an about micrometer diameter's probe. Then, the Pt-Pd film was washed out by aqua regia (HCl and HNO₃ solution with the ratio of 1 to 3). Finally, the diamond probe was attached to a tungsten wire, which was connected to a quartz tuning fork by a silver paste, curing for about 20 minutes at 120 °C.

Figure 1(a) is a SEM (Scanning Electron Microscope) image of the fabricated NV center probe with 2 μm diameter. The PL (Photoluminescence) and ODMR spectrum from the probe were obtained (Fig. 1(b)). Then, a magnetic domain from BLG sample was scanned by the probe. The PL and the ODMR intensity at different points of the sample were imaged (Fig. 1(c)).

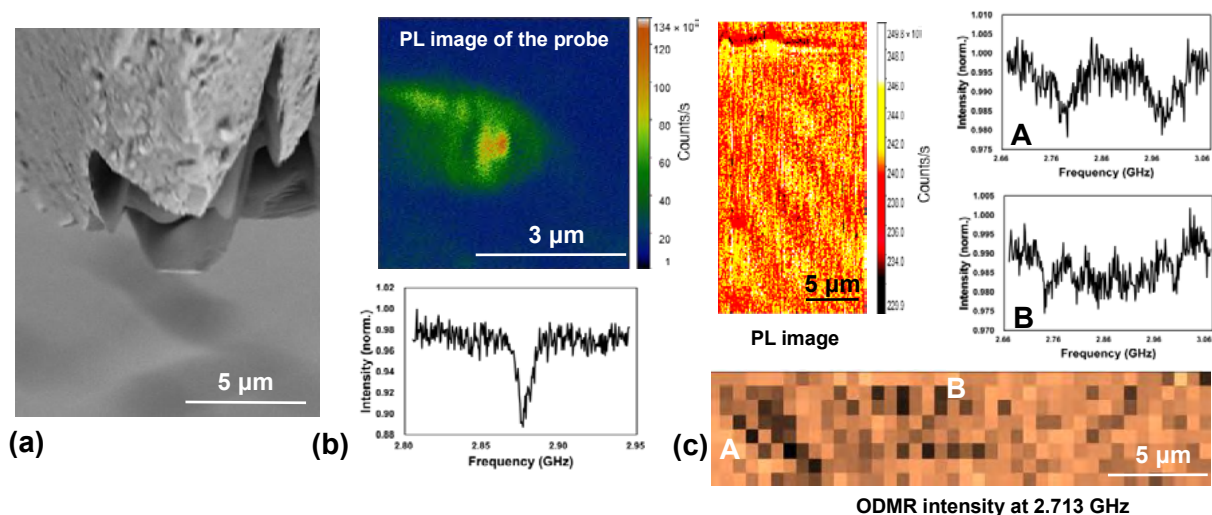


Fig. 1. (a) A SEM image of the FIB-fabricated probe, (b) PL image and ODMR of the scanning diamond probe, (c) PL and ODMR intensity images from the magnetic sample.

Reference:

[1] Y. Kainuma, et al, J. Appl. Phys. 130, 243903 (2021).

Fabrication of scanning diamond NV center quantum sensing probes by using maskless photolithography

Yuma Aoki, Dwi Prananto, Yingshu Ma, Masashi Akabori, Toshi An
School of Materials Science, Japan Advanced Institute of Science and Technology, Japan
Email: s2310001@jaist.ac.jp

In recent years, the artificial synthesis of high-quality diamonds has become possible, leading to high expectations for unprecedented devices employing diamonds. The NV center in diamond is particularly noteworthy, an impurity defect comprising nitrogen (substituted for carbon at the carbon lattice position) and a vacancy created by the missing adjacent carbon atoms. From a sensor perspective, its application as a highly sensitive sensor for magnetic fields, electric fields, temperature, pressure, and other factors is anticipated [1]. Due to its ability to individually observe a single NV center, it can achieve high spatial resolution at the nanometer level. Especially, the scanning NV center probe, which has a nanodiamond pillar at the scanning probe end, can achieve nanometer-scale resolution [2].

The process of making the probe, the pillar fabrication, begins by coating resist to a chemically cleaned diamond sample, followed by light exposure as shown in Figure 1(a). Subsequently, the light-exposed part is removed by immersing it in a developing solution (Fig. 1(b)). Then, nickel is deposited on the sample, and successively Ni layer of a circle shape is removed. After this Ni structure preparation, thermo-chemical etching will be performed, where only the Ni-layered position on the diamond substrate is etched [3], resulting in diamond pillar fabrication (Fig. 1(c)). Once the pillar is fabricated the diamond pillar probe is used as a scanning NV probe.

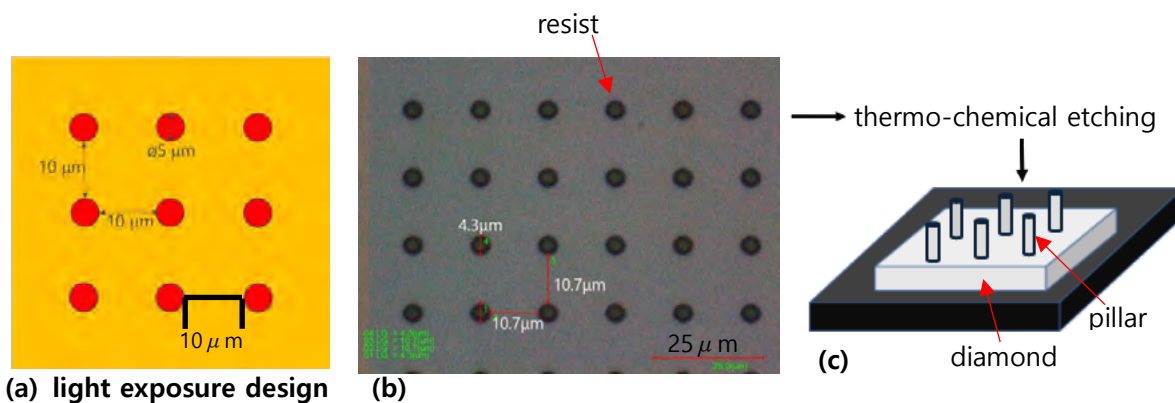


Fig. 1. (a) Light exposure design (Orange area), (b) The surface of the diamond sample after immersion in the developing solution, (c) Schematic at the expected diamond-pillar fabrication.

References

- [1] L. Rondin, Rep. Prog. Phys., **77**, 056503 (26pp), (2014).
- [2] Y. Kainuma, J. Appl. Phys., **130**, 243903 (2021).
- [3] H. Aida, et al., Appl. Phys. Express, **9**, 035504 (2016).

Optimization of spin properties of near-surface NV centers in diamond

Kasane Noda¹, Kun Meng², Dominik B. Bucher², Toshu An¹

¹ School of Materials Science, Japan Advanced Institute of Science and Technology, Nomi-shi, Ishikawa 923-1292, Japan.

² Department of Chemistry, Technical University of Munich, Garching 85748, Germany.

Spin states of the nitrogen-vacancy (NV) centers in diamonds can be detected by optically detected magnetic resonance (ODMR) and time-dependent spin state measurements that are applicable to magnetic sensing and imaging applications at room temperature. We present a study of the spin properties of dense layers of near-surface NV centers in a diamond created by nitrogen (N^{15}) ion implantation. The optically detected Rabi contrast and spin coherence (T_2) time, and spin relaxation (T_1) time, are measured as a function of implantation energy and dose [1]. Here, we study the spin properties of dense near-surface layers of implanted NV centers (overgrown with a 50 nm layer of ^{12}C -enriched material) as a function of implantation energies (2, 3, 4 keV) and doses (1×10^{12} , 3×10^{12} , $1 \times 10^{13} / cm^2$) to identify the optimal conditions for NMR imaging applications.

References:

[1] J. -P. Terienne et al. PHYSICAL REVIEW B **97**, 085402 (2018).

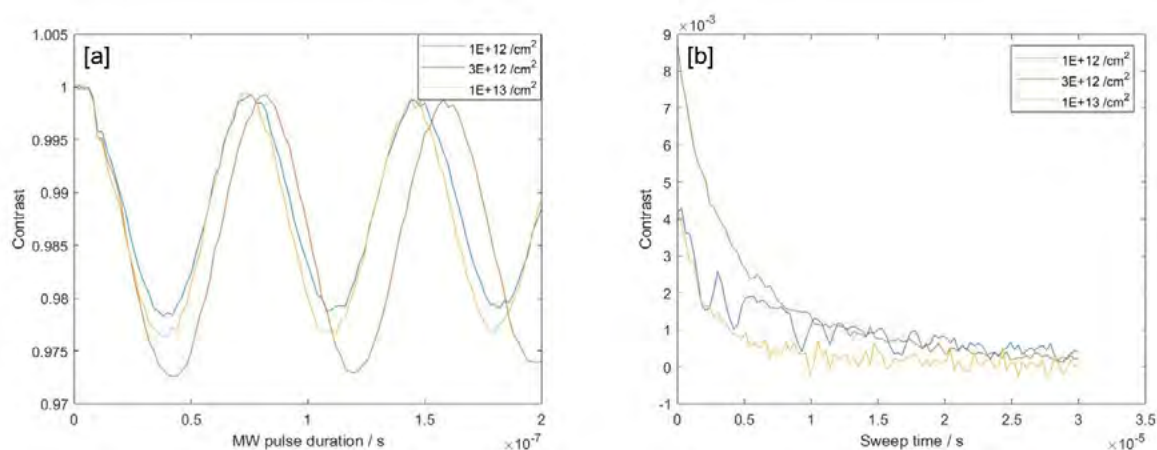


Fig. 1, Rabi oscillation [a] and spin echo (T_2) spectra [b] were obtained with different doses of N^{15} ion implantations energy (3 keV).

Three-dimensional atomic-scale structural characterization of titanium oxyhydroxide nanoparticles by statistical electron microscopy analysis

Kohei Aso¹ and Yoshifumi Oshima¹

¹ Japan Advanced Institute of Science and Technology, Japan.

Since metal hydroxides have various crystal structures even for the same chemical compositions (structural polymorphs), their nanoparticles (NPs) also take polymorphs depending on the synthesis process. The NP's structure can be regarded as defective considering that the surface terminates the crystal lattice periodicity. The defective structure is a reason why structural analysis is difficult by conventional methods such as X-ray diffraction and near-infrared spectroscopy. Metatitanic acid (MA) NPs, composed of titanium (Ti), oxide (O), and hydrogen (H), are one such metal hydroxide. The MA-NPs are widely used as absorbents of uranium, catalysts for organic solvents to absorb carbon dioxides, and precursors for the controlled synthesis of anatase TiO₂ NPs. The structure of MA-NP is similar to anatase TiO₂ [1] but differs because MA includes H elements [2]. Although the structural analysis seems important to understand MAS' properties, the structure is still unclear.

In this study, we have developed an analysis method for obtaining the structure of MA-NPs from projected atomic resolution transmission electron microscopy (TEM) images. Since NPs are dispersed with random orientations on a thin film for the TEM sample, we can obtain the lattice patterns from various projection orientations. To identify the structure from these images, we focused on the plane distances and angles between two specific lattices. These parameters are recorded using fast Fourier transform patterns of images. The procedure is conducted on a thousand NPs in hundreds of HRTEM images assisted by programmed processing.

Structural information was obtained by histograms that show the probability of observing two lattice planes with a certain angular relationship (Figs. 1a and b). The combinations of (101)-(011) and (101)-(004) can be explained by the anatase structure. These two combinations can be observed from [010] and [-1-11], respectively. These results indicate that the base structure is anatase three-dimensionally. In contrast, the lattice plane (002) was observed, which is double periods along the *c*-axis. This (002) is considered to be characteristic of MA-NPs. For further confirmation, typical MA-NP was observed by scanning TEM imaging (Fig. 1c). The contrast of the paired Ti columns shows alternating stacks of the bright (004) and dark (004) planes. This corresponds to the (002) periodicity observed in the TEM analysis. The structural model considered from the growth process suggests alternating layers of anatase TiO₂(004) and H₄TiO₄(004), in which half of the Ti ions are replaced by four H ions [3].

References:

[1] C. Tian, *Sci. Rep.* vol.12, p.20164 (1–12) (2022).

[2] N. Ogata and N. Inoue, *Bull. Soc. Sea Water Sci. Jpn.*, vol.24, p.149–153 (1971).

[3] K. Aso, Y. Oshima, et al., to be submitted.

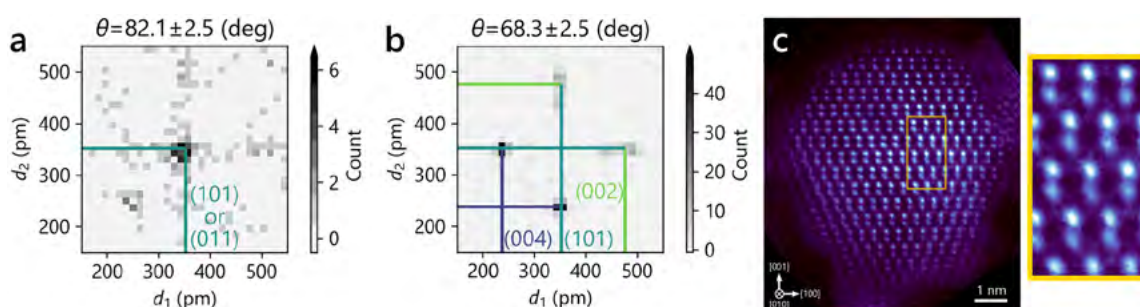


Fig. 1. (a, b) Histograms indicating the probability of observing two lattices with (a) 82 degrees and (b) 68 degrees. (c) STEM image of a typical MA-NP.

First-principles study on structural and electronic properties of FePd/graphene hetero-interfaces

M. Uemoto¹, R. Endo¹, H. Shinya², H. Naganuma³, T. Ono¹

¹ Graduate School of Engineering, Kobe University, Japan.

² Center for Spintronics Research Network (CSRN), The University of Tokyo, Japan

³ Center for Innovative Electronic System (CIES), Tohoku University, Japan.

Magnetic junctions utilizing two-dimensional materials as barrier layers are considered to be alternatives to metal oxide-based barriers such as MgO. This study focuses on the junction consisting of iron palladium (FePd), a ferromagnetic alloy with an L1₀-ordered crystal structure, and graphene (Gr). This FePd/Gr hetero-interface has been recently synthesized using the chemical vapor deposition (CVD) technique. Scanning transmission electron microscopy (STEM) analysis shows that the Fe surface of FePd and Gr layer are bonded and have high crystallinity and flatness [1-2]. Moreover, we have also performed first-principles calculations to investigate interfacial atomic and electronic structures; the proposed model provides stable chemisorbed interfaces and reproduces experimentally measured behaviors [3]. Besides, theoretical models suggest that the magnetoresistance (MR) ratio of FePd/Gr/FePd sandwiched junctions could reach MR = 100~200 [4].

This work also investigates the composition of the alloy surface. Our experimental and theoretical studies indicate that the outermost layer of FePd/Gr predominantly consists of Fe atoms. On the contrary, reports suggest the instability of Fe surfaces in other similar L1₀ alloys without Gr [5]. To address this discrepancy, we propose various models, as shown in Figure. According to the results above, under Gr coverage, the Fe surface model is stabilized owing to the Fe-C interaction, while the Pd surface model remains stable in pristine conditions; this behavior is consistent with previous findings. We also analyzed the effect of the oxidation of the alloy surface. Models with an Fe-O bond in the surface layer exhibit more energetically stable than Pd surface models; this suggests that alloy surfaces in an oxygen environment suppress the formation of the Pd surface. These findings are significant insights for developing high-quality FePd/Gr-based magnetic junctions.

References:

- [1] H. Naganuma *et al.*, Appl. Phys. Lett. **116**, 173101 (2020).
- [2] H. Naganuma *et al.*, ACS Nano **16**, 4139 (2022).
- [3] M. Uemoto, H. Adachi, H. Naganuma, and T. Ono, J. Appl. Phys. **132**, 095301 (2022).
- [4] H. Adachi *et al.* arXiv:2308.02171 [cond-mat.mtrl-sci]
- [5] Y. Taniguchi *et al.* IEEE Trans. Mag., **44**, 11 (2008)

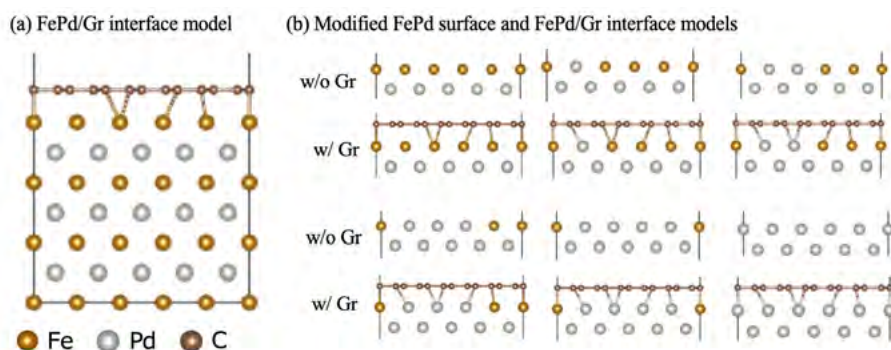


Figure: Computational models

Introduction of microscopic nanomechanical measurement method

Atsuki Uno¹, Jiaming Liu¹, Toyoko Arai², Masahiko Tomitori¹, and Yoshifumi Oshima¹

¹ Japan Adv. Inst. Sci. & Technol., Japan.

² Kanazawa Univ., Japan.

We developed the microscopic nanomechanics measurement method [1], involves integrating a quartz length-extension resonator (LER) as force sensor into the sample holder of a transmission electron microscope (TEM) to investigate the mechanical properties of nanomaterials (approximately 10 nm in size or smaller).

By using LER, the equivalent spring constant of the metal nano-contact can be measured from the change in its resonance frequency, and the energy dissipation produced at the nano-contact can be estimated from the change in the excitation voltage applied to keep its amplitude constant. By evaluating the sensor, the measurement error is about 1 N/m so that it can measure the equivalent spring constant of a metal atomic chain. It means that this method can simultaneously measure elastic and plastic mechanical responses while observing the atomic arrangement of atomic and nanoscale materials by TEM. Using this method, we measured that the Pt atomic chain has a quantized conductance of $2.0 G_0$ ($=2e^2/h$: quantized unit of conductance) and its spring constant is 13.2 N/m. This method is expected to be useful for elucidating the mechanical properties unique to nanomaterials, such as the size and crystallographic orientation dependence of Young's modulus of metallic nano-contacts and so on [1-5].

References:

- [1] J Zhang et al. *Nanotechnology* 31, 205706 (2020).
- [2] J Zhang et al. *Nano Letters* 21, 3922–3928 (2021).
- [3] J. Liu et al., *Appl. Phys. Exp.* 14, 075006 (2021).
- [4] J Zhang et al. *Physical Review Letters* 128, 146101 (2022).
- [5] C. Liu, et al., *Advanced Science* 10 (2023) 202303477.

Estimation of Critical Shear Stress of Au nanocontacts using microscopic nanomechanics measurement method

Jiaming Liu¹, Toyoko Arai², Masahiko Tomitori¹, and Yoshifumi Oshima¹

¹ Japan Adv. Inst. Sci. & Technol., Japan.

² Kanazawa Univ., Japan.

The critical shear stress (CSS) is the stress required for slip to occur on a certain crystal plane, and it is a crucial quantity in understanding material strength. However, the CSS obtained in previous experiments is 2 to 3 orders of magnitude smaller than the theoretical value. This is because there are defects in the bulk sample, which are ignored in theory. Metallic nanocontacts (NCs) with size of a few nanometers are ideal perfect crystalline because of removing the defects. Therefore, measurements of the CSS close to the theoretical values can be expected. We developed the microscopic nanomechanics measurement method [1], involves integrating a quartz length-extension resonator (LER) as force sensor into the sample holder of a transmission electron microscope (TEM). While observing the nanocontact structure in TEM (Figure 1), it allows to measure the electrical conductance, equivalent spring constant, and energy dissipation of the nanocontact simultaneously. The LER is characterized by a high equivalent spring constant ($k_{\text{LER}}=1 \times 10^5$ N/m) and a high resonance frequency (1×10^6 Hz). It can measure the mechanical response of a metal nanocontact bridged between the LER and a fixed electrode with minute amplitudes on the order of tens of picometers [1,2].

We observed the slip deformation of gold nanocontacts in the [110] and [111] directions. We reported the yield stresses (σ) of nanocontacts in the [110] and [111] directions to be 2.0 ± 0.1 GPa and 3.0 ± 0.1 GPa, respectively [3]. Additionally, we measured gold nanocontacts with diameters of 1.9 nm and 2.6 nm, finding no significant differences between them. Theoretical calculations suggest a significant increase in the critical shear stress (CSS) for gold nanocontacts with diameters below 1.5 nm [4]. Therefore, in farther study our purpose is to observe the slip deformation of gold nanocontacts, including those with dimensions smaller than 1.5 nm, and elucidate the size dependence of CSS values.

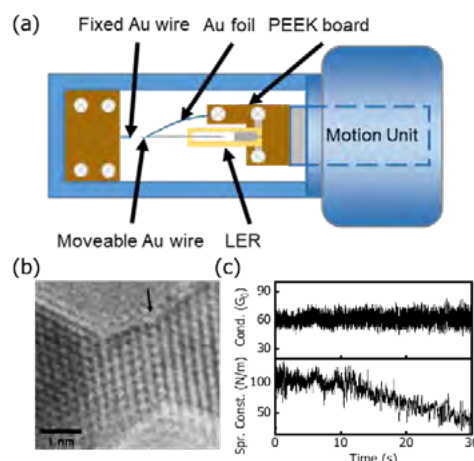


Figure 1 (a) Schematic illustration of the home-made TEM holder. (b) Typical TEM image of Au NC. (c) Time variation of the conductance and the spring constant.

References:

- [1] J. Zhang et al., *Nanotechnology* 31, 205706 (2020).
- [2] J. Zhang et al., *Nano Lett.* 21 3922 (2021).
- [3] J. Liu et al., *Appl. Phys. Exp.* 14, 075006 (2021).
- [4] M. R. Sørensen et al., *Phys. Rev. B* 57, 3283(1998).

Application of large-area CVD-grown few-layer hexagonal boron nitride to magnetic tunnel junction devices

Satoru Emoto¹, Hiroki Kusunose¹, Shunsuke Masuda¹, Satoru Fukamachi²,
Takashi Kimura³, Hiroki Ago^{1,2}

¹ Interdisciplinary Graduate School of Engineering Science, Kyushu University, Fukuoka, Japan

² Global Innovation Center (GIC), Kyushu University, Fukuoka, Japan

³ Graduate School of Science, Kyushu University, Fukuoka, Japan

Hexagonal boron nitride (hBN), a wide-gap 2D insulator, promises many unique applications including insulating layer for 2D devices, deep ultraviolet light emission, single photon emission, gas barrier, and magnetic tunnel junction (MTJ) [1]. Among them, MTJ devices using few-layer hBN as an insulating tunnelling layer are interesting, because the combination of trigonal hBN lattice and fcc(111) ferromagnetic metal electrodes is predicted to give a very high tunnelling magnetoresistance ratio (TMR) [2]. However, the widely used exfoliated hBN flakes are very small, thus limiting development of these devices. Recently, we demonstrated large-scale chemical vapor deposition (CVD) growth of multilayer hBN using Fe-Ni foils and enhancement the carrier mobilities of graphene transistors [3]. In this work, we report selective synthesis of few-layer hBN using thin Fe-Ni films and its application to MTJ devices.

Centimeter-scale, few-layer hBN was grown by CVD at 1200 °C using borazine ($B_3N_3H_6$) feedstock on Fe-Ni films ($Fe_{30}Ni_{70}$) which was deposited on sapphire substrates. We obtained uniform few-layer hBN with a thickness of 1-2 nm. The hBN showed narrow Raman E_{2g} band with a linewidth of 14-16 cm^{-1} and high breakdown voltages of 5-10 MV/cm comparable to exfoliated hBN. These results indicate high crystallinity of our CVD-grown few-layer hBN. With this as-grown hBN, we fabricated MTJ devices by patterning top ferromagnetic electrodes on the hBN surface. Figure 1a illustrates the device structure of the hBN-MTJ. The Fe-Ni catalyst was utilized as a bottom ferromagnetic electrode. The MTJ device exhibited a relatively high TMR of about 10% at 10 K (Figure 1b) [4]. Furthermore, we studied the layer number dependence and found that trilayer hBN gives the highest TMR value (Figure 1c). We can expect further increase of the TMR value by optimizing the metal electrodes and the device structures.

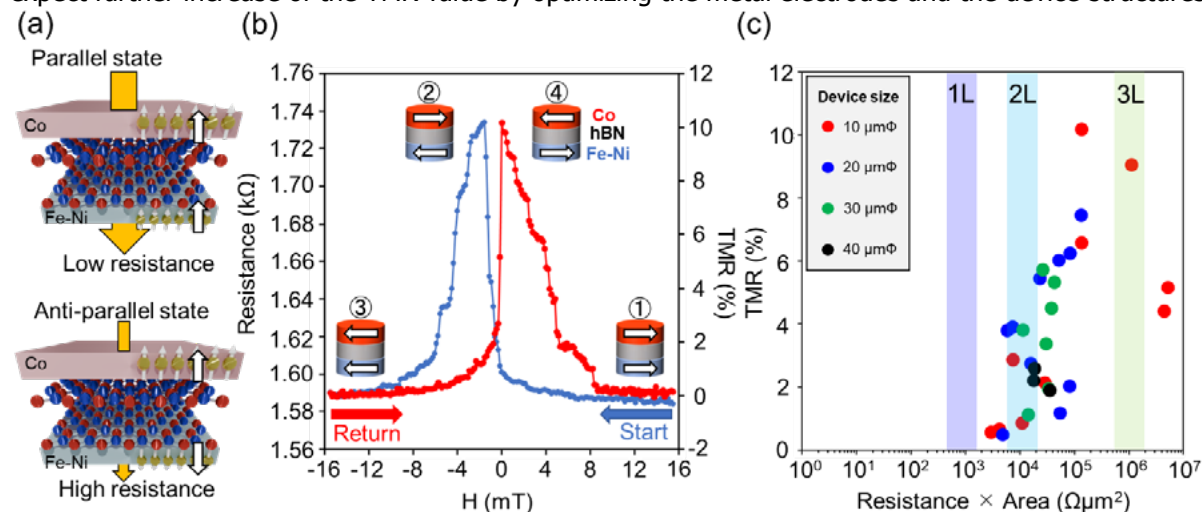


Figure 1 (a) Schematic of a hBN-MTJ device. (b) Device characteristic of few-layer hBN MTJ. (c) Layer-number dependence of the TMR values.

References:

- [1] A. E. Naclerio *et al.*, *Adv. Mater.*, **35**, 2207374 (2023).
- [2] H. Lu *et al.*, *Appl. Phys. Rev.*, **8**, 031307 (2021).
- [3] S. Fukamachi *et al.*, *Nat. Electron.*, **6**, 126 (2023).
- [4] S. Emoto *et al.*, in preparation.

First-principles study on bulk photovoltaic effect in topological insulator phase of halide perovskites

Yedija Yusua Sibuea Teweng¹, Naoya Yamaguchi², Fumiyuki Ishii²

¹ Graduate School of Natural Science and Technology, Kanazawa University, Japan.

² Nanomaterials Research Institute, Kanazawa University, Japan.

Halide perovskites has emerged as one of the promising materials for application on next-generation solar cell devices [1]. In recent years, many theoretical investigations have found that CsPbI₃ may exhibit topological insulator phase under hydrostatic pressure [2]. Previous study suggested that cubic phase of CsPbI₃ exhibited large shift current conductivity around topological phase transition [3]. In this study, we performed density functional theory calculation [4] on tetragonal phase of CsPbI₃. Using Wannier90 calculation [5,6], we evaluated the shift current conductivity under hydrostatic pressure. We found the CsPbI₃ tetragonal phase undergo the paraelectric to ferroelectric phase beyond pressure 5 GPa. In addition, the topological phase transition from trivial to non-trivial states on electronic structure is found for the pressure larger than 8 GPa. We found the shift current conductivity is significantly enhanced as the pressure is increased. Therefore, it is expected that this result may stimulate the investigation of high-pressure experiment on shift current mechanism in ferroelectric halide perovskite.

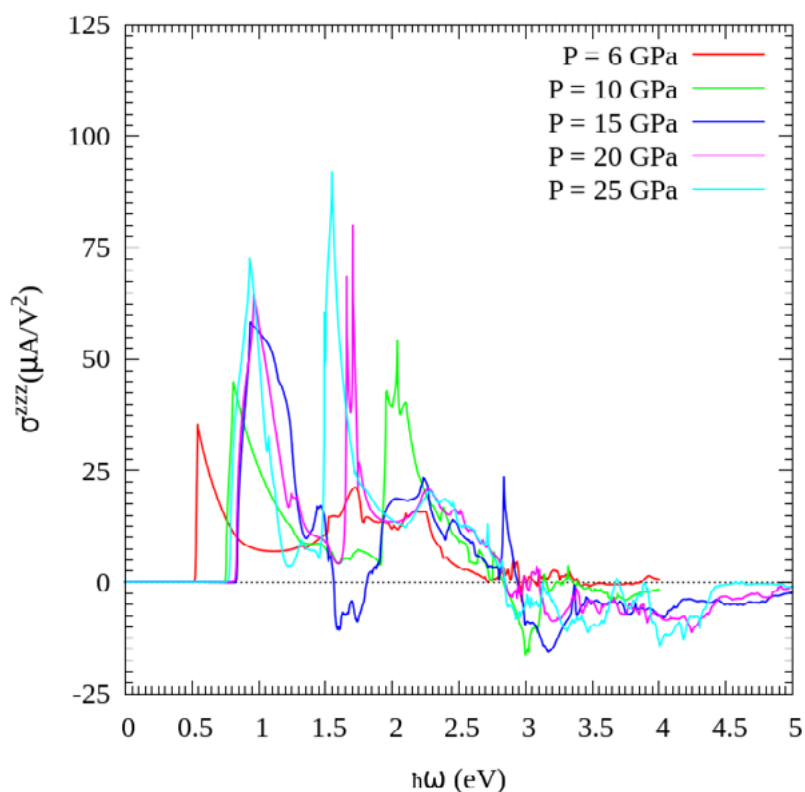


Fig 1: Calculated shift current conductivity of CsPbI₃ tetragonal phase under hydrostatic pressure.

References:

- [1] Dong, C.Ran, W.Gao, M.Li, Y.Xia, W.Huang: eLight. **3**, 3 (2023).
- [2] S. Liu, Y. Kim, L. Z. Tan, A. M. Rappe. Nano Lett. **16**, 1663 (2016).
- [3] L.Z Tan and A.M Rappe. Phys.Rev.Lett. **116**. 237402 (2016).
- [4] T. Ozaki and H. Kino. Phys.Rev.B. **69**. 195113 (2004)
- [5] G. Pizzi, et.al. J.Phys.Cond.Matt. **32**, 165902 (2020).
- [6] J.I. Azpiroz, S.S. Tsirkin and I. Souza, Phys.Rev.B, **97**. 245143 (2018).

Transferable high- k /boron nitride gate dielectric for 2D field-effect transistors

Eui Young Jung¹, Pablo Solís-Fernández², Keisuke Yamamoto¹, and Hiroki Ago^{1,2}

¹ Interdisciplinary Graduate School of Engineering Science, Kyushu University, Fukuoka, Japan

² Global Innovation Center (GIC), Kyushu University, Fukuoka, Japan

Two-dimensional (2D) materials have attracted great interest due to their unique structures and exceptional physical properties, making them promising candidates for electronic and photonic applications. Among them, hBN stands out as a wide gap insulator (~ 6 eV) with atomically flat surface and high chemical stability and mechanical strength. Although hBN is widely used as a gate insulator for transistors of semiconducting 2D materials like transition metal dichalcogenides (TMDCs), the dielectric constant of hBN is not as high as that of high- k materials, such as Al_2O_3 and HfO_2 [1]. These high- k materials can be deposited by atomic layer deposition (ALD) to use as the gate dielectric for 2D-based devices [2]. However, the inert and flat surfaces of 2D materials often result in non-homogeneous ALD films, and 2D materials suffer damages during the ALD process [3].

In our study, we employed CVD-grown, large-area multilayer hBN [4-6] as a sacrificial layer for an Al_2O_3 film made by the ALD, rather than depositing Al_2O_3 directly onto the 2D material of the device channel (Figure 1). This strategy effectively circumvents potential damage to the 2D material during the ALD process. In addition, this approach allows us to transfer high- k materials onto TMDC without giving damages in top-gate field-effect transistors (FETs). We studied various modifications of the hBN surface and found that UV ozone (UVO) treatment is effective for this purpose. As shown in Figure 2, we could obtain very flat and uniform Al_2O_3 film on the modified hBN surface, while on the pristine (untreated) hBN inhomogeneous deposition of Al_2O_3 was observed. Our work will enable the production of gate dielectrics with high dielectric constants and low leakage current, contributing to the development of high-performance TMDC transistors.

References:

- [1] T. Knobloch *et al.*, *Nat. Electron.*, **4**, 98 (2021). [2] K. Zhou *et al.*, *PRL*, **105**, 126601 (2010). [3] S. McDonnell *et al.*, *ACS Nano*, **7**, 10354 (2013). [4] Y. Uchida *et al.*, *ACS Nano* **12**, 6236 (2018). [5] Y. Uchida *et al.*, *ACS Appl. Electron. Mater.* **2**, 3270 (2020). [6] S. Fukamachi *et al.*, *Nat. Electron.* **6**, 126 (2023).

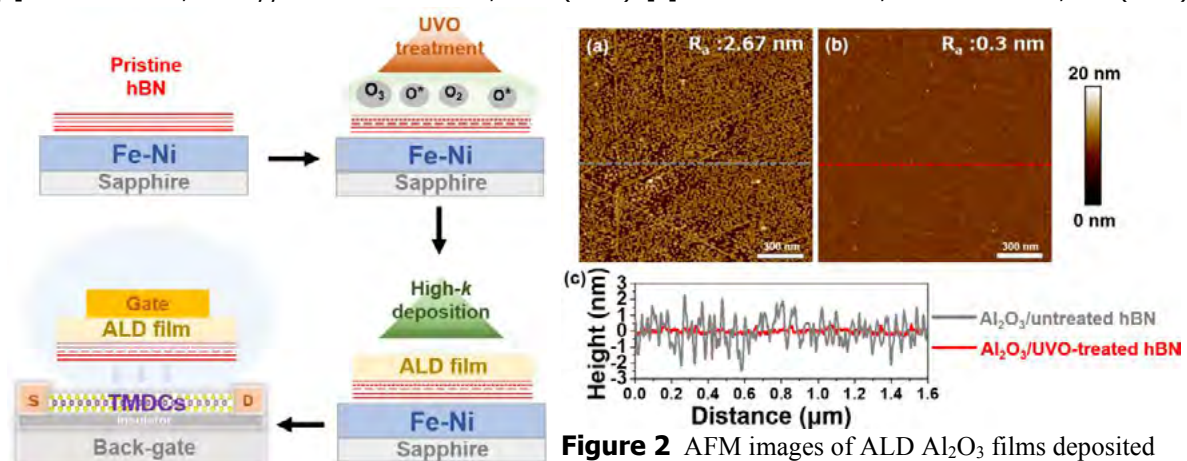


Figure 1 Schematic of the fabrication of top-gate 2D-FET using a transferable ALD/hBN insulating stack.

Figure 2 AFM images of ALD Al_2O_3 films deposited on untreated hBN (a) and UVO-treated hBN (b). (c) Height profiles of the Al_2O_3 /untreated hBN (gray) and Al_2O_3 /UVO-treated hBN (red).

Enhanced superconductivity by intrinsic strain in NbTe₂

Takaya Shimokawa¹, Hayato Makino¹, Kaito Sato¹, Kazutoshi Shimamura², Yukiko Obata¹, Hiroyuki Okamoto³ and Yasuo Yoshida¹

¹ Department of Physics, Kanazawa University, Kanazawa, Ishikawa 920-1192, Japan.

² Institute of Science and Engineering, Kanazawa University, Kakuma-machi, Kanazawa, 920-1192, Japan.

³ School of Health Sciences, Kanazawa University, Kanazawa 920-0942, Japan.

The transition metal dichalcogenides (TMDCs), which are quasi-two-dimensional materials and have layered structure coupled with weak van der Waals force, attract much attention because of their unique two-dimensional properties different from bulk. 1T''-NbTe₂, which belongs to TMDCs, has a charge density wave transition above room temperatures and a superconducting transition at 0.5 K. We grew 1T''-NbTe₂ samples using chemical vapor transport method with two different growth procedures, resulting in two types of samples: one with a superconducting temperature (T_c) at 0.5 K and one with T_c at 2.8 K which is three times higher than the other. Our chemical analysis shows that both samples show no significant difference in the chemical compositions. The sample with enhanced superconductivity does not show magnetoresistance while the standard one shows the typical magnetoresistance of NbTe₂. This indicates a multi-domain character of the enhance T_c sample and Laue X-ray method also suggests the same conclusion. Single-crystal X-ray analysis reveals that the unit cell volume of samples with enhanced T_c expands by 1% compared with the standard sample due to the intrinsic strain, as shown in Table 1. This intrinsic strain is a possible origin for the enhanced superconductivity since it can modify the band structure and the density of states at \bar{E}_F . In the presentation, we will report the details of our experimental results of the standard and the T_c enhanced NbTe₂.

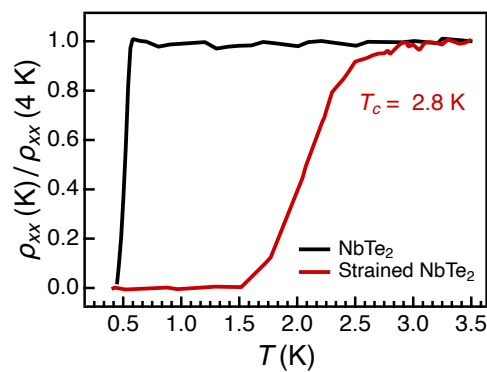


Figure 1. Resistivity of two types of NbTe₂ samples.

Parameter	NbTe ₂	Strained NbTe ₂
a (Å)	19.44	19.276
b (Å)	3.645	3.673
c (Å)	9.327	9.313
β (°)	134.58	133.87
Interlayer distance (Å)	6.643	6.711
Unit cell volume (Å ³)	470.65	475.65

Table 1. Lattice parameters and unit cell volume of the standard and strained NbTe₂ samples.

References:

[1] E. Brown, Acta Crystal. 20, 264 (1966).

Precise measurement of ripple structure of MoS₂ nanoribbon when stretching

Wei Xiong, Limi Chen, Lilin Xie, Kohei Aso and Yoshifumi Oshima

School of Materials Science, Japan Advanced Institute of Science and Technology, 1-1 Asahidai, Nomi, Ishikawa, 923-1292, Japan

Ripple structure in 2D materials was formed when stretching or suppressing along certain directions. Although the amplitude and the period of the ripple structure has been reported to depend on the strain for relatively large scales such as 100 nm to 1 μm , it has not been investigated for very thin 2D materials in atomic scale experimentally. Recently, Xie et al, successfully measured the atom-scaled amplitude and period for the rippled structures of molybdenum disulfide (MoS₂) flakes by applying geometrical phase analysis (GPA) method to atomically resolved transmission electron microscope (TEM) images [1,2]. However, there were problems such that the gap for suspending the nanoribbon was wide (larger than 1 μm) and the height difference was large between both terminals to suspend very thin nanoribbon such as monolayer at the gap.

In this study, we developed a new method to make the gap for suspending very thin MoS₂ nanoribbon and investigated the strain dependence of the amplitude and the period of the ripple structure for the MoS₂ nanoribbon.

We used the silicon chip coated by silicon nitride (SiN) film of 400 nm in thickness. The gap was formed by cutting along a line in the window of the SiN film for TEM observation using a focused ion beam (FIB), which width was about 200 nm. Exfoliated thin MoS₂ flake was then picked up by polypropylene carbonate (PPC)/polydimethylsiloxane (PDMS) stamp using a dry transfer method. A target MoS₂ flake can be picked up precisely by the strong adhesive force of the stamp. Due to the thermoplastic property of PPC, the adhesion force of the stamp decreases by heating up to 70-90 $^{\circ}\text{C}$. Therefore, by controlling the relative position of the flakes to the gap and the temperature of the stamp while observing with an optical microscope, the flakes could be positioned so that they were suspended on both sides of the gap. The atom-scaled ripple structure of the MoS₂ nanoribbon was observed by a homemade TEM holder, which enable us to be stretched by a piezo actuator. The stretch distance was confirmed to be almost in proportional to the bias voltage applied to the piezo.

We found the periodic modulation, which was formed along the armchair direction, in the TEM image as shown in Fig. 1. In the areas indicated by red dashed boxes, the atomic columns are not clearly visible because the atoms do not overlap in the column. In some regions, the lattice contrast does not match with the yellow hexagonal array, which shows the ideal arrangement of the atomic columns, due to local modulation of lattice spacing. These features could be explained by a ripple structure. By analyzing TEM images using GPA, the period and amplitude of the ripple structure could be estimated precisely.

References:

[1] L. Xie and Y. Oshima, *Nanotechnology* 32, 185703 (2021).

[2] L. Xie and Y. Oshima, *Appl. Surf. Sci.* 597, 153708 (2022).

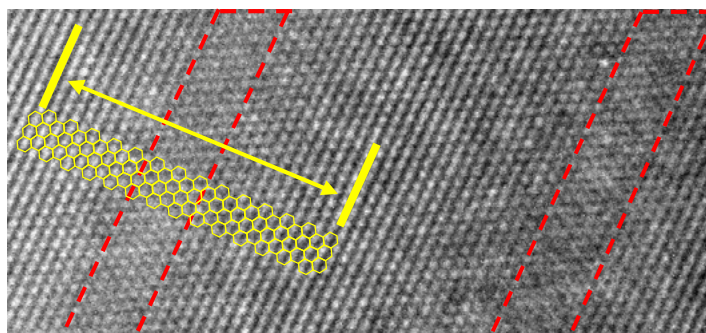


Figure 1 An atom-resolved TEM image of the rippled MoS₂

Electrical conductance of suspended MoS₂ nanoribbon measured by in-situ transmission electron microscope

Limi Chen¹, Chunmeng Liu¹, Fayong Liu¹, Kareekunnan Afsal¹, Hiroshi Mizuta¹ and Yoshifumi Oshima¹

¹ School of Materials Science, Japan Advanced Institute of Science and Technology, Nomi, Ishikawa, 923-1292, Japan.

Monolayer MoS₂ is a direct transition semiconductor with a wide bandgap of 1.8 eV, which is expected to be applied to nanodevices. The field-effect transistor (FET) based on monolayer MoS₂ nanoribbon has presented a high on/off ratio of over 10⁸ with ultra-low power dissipation, [1] making them attractive for high-efficiency switching and logic circuits. Recently, the novel properties exhibited by the edge states of monolayer MoS₂ nanoribbons have attracted much attention, which has been also suggested to be apparent when the width of the nanoribbon becomes narrower. However, the effect of the edge effect on the nanoribbon width has not been well elucidated due to the difficulty of conducting experiments.

In-situ transmission electron microscopy (TEM) is a powerful method [2,3]. In this study, we aim to elucidate the relationship between the widths and the electrical conduction properties of MoS₂ nanoribbons by developing the in-situ TEM method. For this purpose, we established a dry transfer method to transfer nanometer-sized monolayer MoS₂ flake to suspend between metal electrodes on the silicon chip, as shown in Figure 1. Compared to conventional lithography processes, our method has the advantage of keeping the nanoribbon clean and making less introduction of strain and defects. As the transfer stamp, we selected polypropylene carbonate (PPC), whose thermoplastic properties help reduce the transfer pressure through temperature control. We successfully transferred 300nm-wide MoS₂ nanoribbon to suspend between 10μm-wide electrodes and removed the residual contaminants on the nanoribbon by annealing in an Ar/3% H₂ atmosphere for 1h. It was then mounted on the in-situ TEM holder and narrowed down by sculpting of intense electron beam irradiation. The MoS₂ nanoribbon was observed simultaneously with measuring the current-voltage (I-V) curves during the thinning process, as shown in Figure 2. We think that the electrical conduction properties of the MoS₂ nanoribbon are not obtained clearly due to the high contact resistance with the electrode. By improving this point, we will clarify the width dependence of electrical conduction.

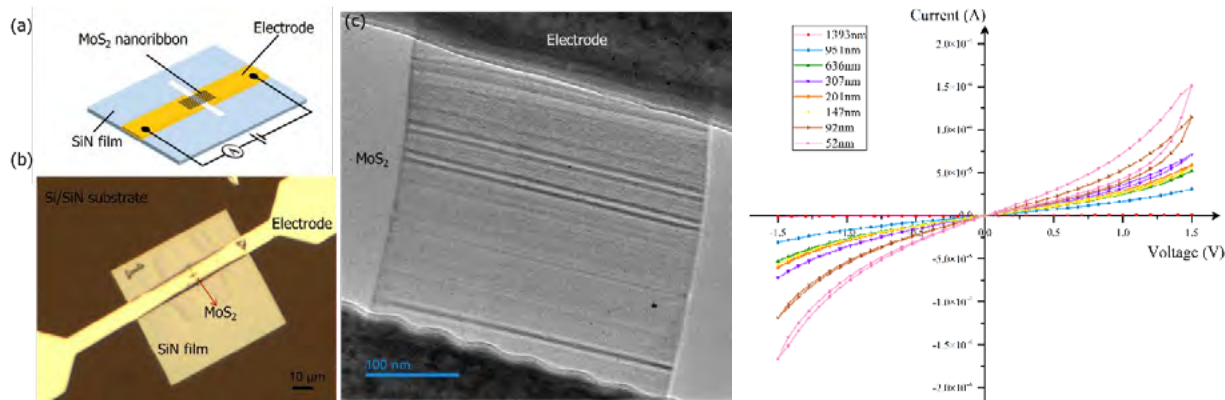


Figure 1 (a) The schematic illustration of the self-made device [3]. (b) Optical image of suspended MoS₂ nanoribbon device. (c) TEM image of initially 300nm wide MoS₂ nanoribbon device. Figure 2 Several I-V curves of the MoS₂ nanoribbon with different widths taken from the thinning process.

Reference:

- [1] Radisavljevic, B., Radenovic, A., Brivio, J., Giacometti, V., & Kis, A. (2011). Nature nanotechnology, 6(3), 147-150.
- [2] Liu, C., Zhang, J., Muruganathan, M., Mizuta, H., Oshima, Y., & Zhang, X. (2020). Carbon, 165, 476-483.
- [3] Liu, C., Zhang, J., Zhang, X., Muruganathan, M., Mizuta, H., & Oshima, Y. (2020). Nanotechnology, 32(2), 025710.

In-situ TEM observation of effect of electron irradiation on electrical conductance in GaSe films

Mai Nakashima¹, Limi Chen¹, Kodai Fukumoto¹, Kohei Aso¹, Yukiko Takamura-Yamada¹, Yoshifumi Oshima¹

¹ Japan Advanced Institute of Science and Technology, Ishikawa 923-1292, Japan

Miniaturization of electronic devices is required to promote integration and reduce power consumption. It is one of hot topics in materials science to explore nanoscale semiconducting materials such as two-dimensional nanoribbons that are expected to exhibit specific properties when they are made thinner or smaller. Recently, the electrical conductance of monolayer tungsten sulfide (WS₂) nanoribbon has been reported to reveal a reversible decrease in conductivity with increasing beam current density when it was irradiated by electron beam in transmission electron microscopy (TEM). Gallium selenide (GaSe) is known to be a highly photo-responsive two-dimensional material.

In this study, in order to clarify the effect of electron irradiation on the electrical conduction of very thin GaSe nanoribbons, we conducted in-situ TEM experiment. We tried to clarify the electron beam irradiation effect on thin GaSe (band gap: 2.0 eV) nanoribbons by measuring their current-voltage (I-V) characteristics with different dose of the electron beam irradiation in the TEM.

The devices of suspended GaSe nanoribbons were fabricated as follows: GaSe nanoribbons mechanically exfoliated from single crystals were suspended between electrodes to obtain I-V characteristics while observing TEM [2,3]. Thin Au electrodes (width: 5-15 μm) were fabricated by vapor deposition on a Si/SiN substrate with a window for TEM observation, and the GaSe flakes were transferred to be suspended at the gaps, which were made by focused ion beam fabrication.

[1] Y. Fan, ACS Appl. Mater. Interfaces 8 (2016) 32963.

[2] C. Liu, Carbon 165, 476-483 (2020).

[3] C. Liu, Nanotechnology 32, 025710 (2020).

Electron trap prediction based on solid-state electronic structure for lanthanide ions doped CaCO₃ phosphors

Hirohisa Miyata¹, Jumpei Ueda¹,¹Japan advanced institute of science and technology, JAPAN

Persistent phosphors are optical-functional materials that continue to emit light for several seconds to several hours even after ceasing excitation. They are commonly employed in applications such as emergency signage and clock dials. Persistent luminescence originates from capturing the optically generated electrons or holes with crystal defects. Subsequently, under ambient temperature, the captured electrons or holes gradually release and migrate toward luminescent centers, thereby sustaining long-lasting luminescence. While numerous reports exist on persistent phosphors utilizing aluminate-based or silicate-based compounds like SrAl₂O₄:Eu²⁺-Dy³⁺ and Sr₂MgSi₂O₇:Eu²⁺-Dy³⁺, there has been limited development on persistent phosphors employing carbonate compounds. Recently, CCUS (carbon capture, utilization, and storage) technologies have been attracted to achieve a carbon-neutral society by managing and utilizing carbon dioxide, a greenhouse gas. Consequently, the development of persistent phosphors utilizing carbonate-based materials derived from carbon dioxide offers the potential for high-value optical functional materials, contributing to the realization of CCUS. Therefore, this study investigates the feasibility of carbonate compounds as persistent phosphor hosts by fabricating various rare-earth-doped CaCO₃ phosphors, analyzing the solid-state electronic structure and predicting electron traps through analysis.

CaCO₃:0.5%Eu³⁺-0.5%Li⁺, CaCO₃:0.5%Eu²⁺, and CaCO₃:0.5%Ce³⁺ were synthesized by coprecipitation method. Starting materials such as CaCl₂·2H₂O (3N), CeCl₃·7H₂O (3N), EuCl₃·6H₂O (4N), and (NH₄)₂CO₃ were adjusted to 1M aqueous solutions. The rare-earth elements (RE = Ce, Eu) and calcium mixed chloride solutions were continuously stirred while (NH₄)₂CO₃ solution was added dropwise. The resultant precipitates were centrifuged and dried at 80°C under ambient atmospheric conditions. Samples were heat-treated at 700°C in CO₂ atmosphere for 6h. Additionally, thermal treatments were conducted, if required, by mixing Li₂CO₃ (3N) as a charge compensator and 10wt% NH₄Cl (99.5%) as a reducing agent.[1] The crystalline phases of the prepared samples were identified using powder X-ray diffraction (XRD), and various optical measurements were conducted on the samples after heat treatment.

Based on the XRD pattern (Fig. 1), it was confirmed that the as-precipitated sample consisted of a mixture of CaCO₃ polymorphs, vaterite and calcite, and the heat-treated samples were identified as calcite phases [2, 3]. Fig.2 illustrates the photoluminescence emission and excitation spectrum of each sample at room temperature. The CaCO₃:Ce³⁺ sample showed a broad emission band around 350–400 nm, which is attributed to the 5*d*-4*f* transition of Ce³⁺. In CaCO₃:Eu³⁺-Li⁺, emission peaks related to the 4*F*-4*F* transition of Eu³⁺ were observed around 550-750 nm. CaCO₃:Eu²⁺ displayed a single emission band around 400–450 nm attributed to the 5*d*-4*f* transition of Eu²⁺, with a bandwidth of 25 nm. We also investigated the PLE spectra in vacuum ultraviolet (VUV) region and determined the host exciton energy and charge transfer energy related to Eu³⁺. Utilizing the obtained spectral data and the proposed energetic model[4], vacuume referred binding energy (VRBE) diagram was constructed to predict the trap depth by trivalent lanthanide dopants.

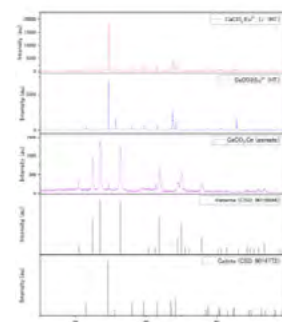


Figure 2 XRD pattern of CaCO₃ samples.

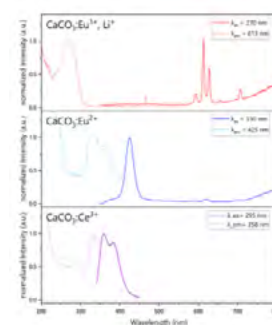


Figure 2 PL / PLE spectra of RE-doped CaCO₃ samples

[1] Y.Kojima, S.Doi and T. Yasue, *J. Ceram. Soc. Jpn.*, **111** [5], 343–347 (2003) [2] S. M. Antao and I. Hassan, *Can. Mineral.*, **48**, 1225–1236 (2010) [3] A. Le Bail, S. Ouhenia and D. Chateigner, *Powder Diffr.*, **26**, 16–21 (2011) [4] P.Dorenbos, *Phys. Review B*, **85**, 165107 (2012)

Double Electron-Electron Resonance Spectroscopy by Using a Scanning Nitrogen Vacancy Center Diamond Probe

¹Thitinun Gas-osothe, Dwi Prananto, Kunitaka Hayashi, Toshu An

¹School of Materials Science, Japan Advanced Institute of Science and Technology, Japan

Email: s2120405@jaist.ac.jp

Double electron-electron resonance (DEER) is the method to measure the interaction between the coupling of at least two electrons which are at a different distance in nanometer range. This spin interaction can be observed in time domain shortening the spin echo decay. In this research, we demonstrate the double electron-electron resonance of nitrogen-vacancy (NV) pattern diamond sensing by using a laboratory ensemble NV diamond probe as a sensor, which is fabricated by using an electronic grade (EG) type-II diamond with (100) orientation. The diamond was implanted with nitrogen to form the NV defect in the diamond structure. In figure 1(a), the focus ion beam (FIB) was used to carve a 1 μm diameter tip in the NV diamond. In the target sample in Figure 1(b), the nitrogen ions at 30 keV and a dose of 1×10^{12} ion/cm² were used to implanted into the bulk EG diamond with (001) orientation from the Element Six company which was covered by a $6.5 \times 6.5 \mu\text{m}^2$ copper gilder as a mask. This energy of implantation is used to estimate the NV center depth of about 30 nm from the surface. The electron spin resonance (ESR) of the NV diamond probe and diamond target are measured by optically detected magnetic resonance (ODMR). In a certain external magnetic field, the spin dependent frequencies from the Zeeman effect of the NV probe and target are split separately because of a different orientation (see Figure 1(c)). Due to the environmental interaction, the spin echo was exploited to identify the coherent time, T_2 .

In DEER experiment, the target spins of the NV pattern diamond are manipulated by adding the second microwave π -pulse at the Larmor frequency, which is associated with the external magnetic field, in the middle of spin echo pulse sequence. Meanwhile, the spin direction of the target is inverted and causes the reverse dipole-dipole interaction of the electrons between NV probe and NV target [1]. This reverse dipole fields disorder the spin echo decay, then the shortened T_2 is observable (see Figure 1(d)).

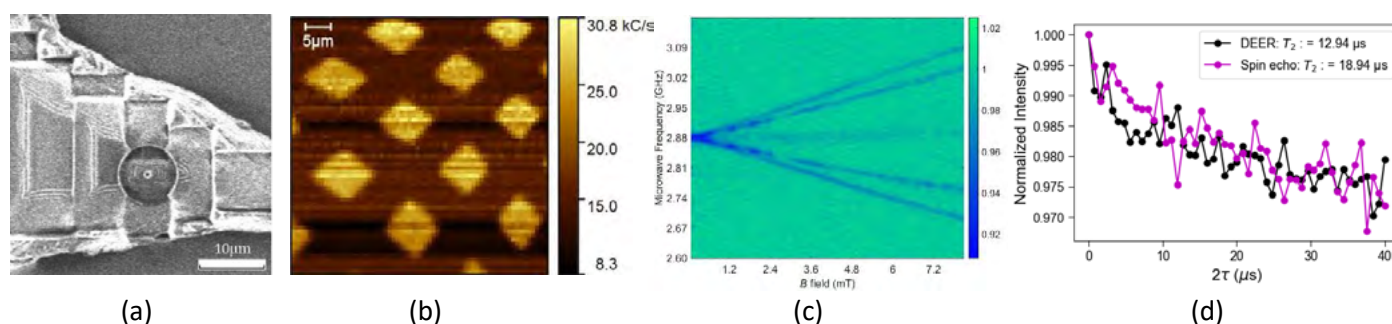


Figure 1. (a) NV diamond probe fabrication in FIB. (b) Fluorescence of NV pattern on the bulk EG diamond. (c) Frequency split magnetic field dependence of the NV probe and NV target. (d) DEER and Spin echo results with coherent time decay, T_2 .

Reference:

[1] H. Mamin, M. Sherwood, and D. Rugar, "Detecting external electron spins using nitrogen-vacancy centers," *Physical Review B*, vol. 86, no. 19, p. 195422, 2012.

Temperature detection using a scanning diamond NV center probe for thermal imaging

Kunitaka Hayashi¹, and Toshi An¹

¹ School of Materials Science, Japan Advanced Institute of Science and Technology, Japan.

E-mail: kuni-hys@jaist.ac.jp

The nitrogen-vacancy center (NV center) is a defect structure in the diamond, that can measure the magnetic field, electric field, and temperature. It has been attracting attention from various fields in recent years [1]. Temperature detection is performed by measuring the optically detected magnetic resonance (ODMR), where the ODMR dip frequency shifts depending on temperature [2-3].

There exist thermal imaging methods such as thermo-reflectance thermal imaging, but its resolution is limited by the wavelength of the light and may not be sufficient for applications such as the analysis of miniaturized semiconductor circuits. The application of scanning diamond NV center probe to an atomic force microscope (AFM) will enable temperature measurement with nanoscale spatial resolution. In this study, we report on the temperature measurement method using a scanning diamond NV center probe.

The scanning diamond NV center probe was prepared by attaching a pyramidal shape of the diamond with an ensemble NV center about 10 μm length attached to a quartz crystal tuning fork via a tungsten wire with epoxy glue. The radius of curvature of the diamond apex is estimated to be several hundred nanometers. The ODMR spectra shifts of the scanning diamond NV center probe were measured by monitoring a silicon sample temperature with a thermometer, where the sample temperature was controlled by a Peltier device. The isolated pyramidal-shaped diamond was also put on the sample directly to compare with that of the scanning NV probe. The frequency shift of the ODMR showed differently between the scanning NV probe and the isolated pyramidal diamond, especially at high-temperature conditions (Fig1 d).

References:

- [1] J.-P. Tetienne, et al, Science 20, **344**, 1366 (2014)
- [2] V. M. Acosta, et al, PRL **104**, 070801 (2010)
- [3] M. Fujiwara, et al, Phys. Rev. Research **2**, 043415 (2020)

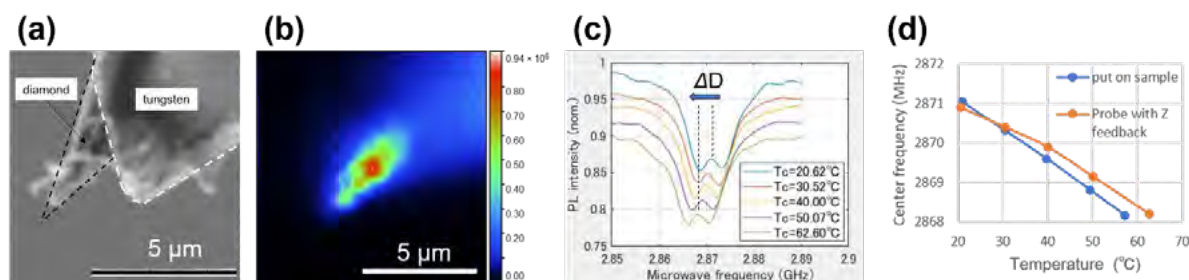


Fig.1 (a) Side view SEM image of the scanning diamond NV center probe. (b) Top view Photoluminescence image of the scanning diamond NV center probe. (c) The scanning diamond NV center probe ODMR spectra shift lower frequency as a function of the temperature increase. (d) Differences in the slope of the frequency shift between a diamond put on a sample and scanning diamond NV probe.

First Principles Study of Electron and Phonon in BaSi₂ Polymorph

Zohan Syah Fatomi¹, Fumiyuki Ishii²

¹ Graduate School of Natural Science and Technology, Kanazawa University, Kakuma-machi, Kanazawa-shi, 920-1192, Japan

² Nanomaterials Research Institute (NanoMaRI), Kanazawa University, Kakuma-machi, Kanazawa-shi, 920-1192, Japan.

Thermoelectric material offers sustainable energy conversion which is crucial for industrial heat waste^[1]. Recent studies show that silicon-based materials are gaining much attention due to their abundant availability (low cost), non-toxicity, and compatibility with thermoelectric^[2]. Here we propose BaSi₂ (EuGe₂-type and SrSi₂-type) as the promising candidate for thermoelectric material^[3]. The first principles study based on generalized gradient approximation (GGA) is performed using PHASE/0 DFT code^[4]. We study the stability properties, electronic structure, and phonon dispersion of EuGe₂-type and SrSi₂-type in BaSi₂. The DFT calculations show that the EuGe₂-type and SrSi₂-type have stable trigonal and cubic crystal structure configurations, respectively. The electronic structure calculations show that both EuGe₂-type and SrSi₂-type possess semimetals characteristics which are expected to have good potential for thermoelectric application. When SOC is included, it is found that there are strong band splittings at SrSi₂-type (point of G-X) while the VBM and CBM at EuGe₂ are expected to get closer to each other (point of L-H). The SOC is expected to have an important role in affecting thermoelectricity quality for both EuGe₂-type and SrSi₂-type^[5]. The calculation of phonon dispersion shows that there is no imaginary frequency for both EuGe₂-type and SrSi₂-type indicating that EuGe₂-type and SrSi₂-type have excellent dynamic stability. It is also found that the maximal acoustic vibration frequency in EuGe₂-type is 3.02 THz which is expected to be beneficial for low thermal conductivity^[6].

Keywords: BaSi₂, band structure, spin-orbit coupling, phonon, density functional theory

References:

- [1] H. Mamur, et al. *Cleaner Materials*. **2**. 100030 (2021).
- [2] K. Hashimoto. *J. Appl. Phys.* **102**. 063703 (2007).
- [3] J. Evers. *Journal of Solid State Chemistry*. **32**. 77-86 (1980).
- [4] PHASE/0. First-principles Electronic Structure Calculation Program. <https://azuma.nims.go.jp/> .
- [5] M.Z. Mohyedin, et al. *Computational & Theoretical Chemistry*. **1182**. 112851 (2020).
- [6] S. Guo and L. Qiu. *J. Phys. D: Appl. Phys.* **50**. 015101 (2016).

Application of Machine Learning in High-Throughput Screening of 2D Materials for Transverse Thermoelectric

Akmal Fauzi¹, Rifky Syariati², Fumiyuki Ishii²

¹ Graduate School of Natural Science and Technology, Kanazawa University, Kakuma, Kanazawa, 920-1192, Japan.

² Nanomaterials Research Institute (NanoMaRi), Kanazawa University, Kakuma, Kanazawa 920-1192

In a 2D system, the use of 2D materials decreases thermal conductivity (κ) through surface phonon scattering¹. Electrical conductivity σ increases due to weak electron-lattice interaction in 2D materials caused by restricted phonon-electron scattering channels². By using transverse thermoelectricity phenomenon, the flexible TE devices can be achieved³. Transverse thermoelectricity, linked to anomalous Hall and Nernst conductivity, allows flexible TE devices with 2D magnetic materials like CrI₃, CrGeTe₃, Fe₃GeTe₂, and VSe₂. High-throughput calculations predict new 2D magnetic materials, as demonstrated in our previous work building databases for transverse TE properties of 2D magnetic materials through high-throughput density functional calculations.

The available data is valuable for application in machine learning, offering a solution for prediction to reduce computational costs and facilitating data analysis for new insights. Various machine learning methods, including regression, classification, clustering, and others, can be employed. Initiating the process with data visualization or exploratory data analysis often yields valuable insights. An example involves mapping anomalous Hall conductivity versus density of states at the Fermi level to classify insulators, metals, and magnetic topological materials (Chern insulators). Additionally, mapping anomalous Nernst conductivity at the Fermi level versus density of states reveals insights such as the largest α_{xy} around -160 ((e²/h)(μ V/K)) with a corresponding density of states of 2.25 ((state/eV)/nm²) at 100 K. Some 2D magnetic structures exhibit substantial α_{xy} , exceeding |300| ((e²/h)(μ V/K)) by tuning μ through mapping the chemical potential dependence of anomalous Nernst conductivity maximum.

For further research, mapping will be extended to explore additional properties, and machine learning techniques will be employed for classification and clustering of various materials. Furthermore, the utilization of machine learning for predicting several properties will involve incorporating crystal structure information and other relevant data.

Keywords : Machine Learning, 2D Materials, Transverse Thermoelectric, Density Functional Theory

References:

[1] Anufriev, R., Maire, J. and Nomura, M. (2016) 'Reduction of thermal conductivity by surface scattering of phonons in periodic silicon nanostructures', *Physical Review B*, 93(4). doi:10.1103/physrevb.93.045411.

[2] Lee, M.-J. et al. (2016) 'Thermoelectric materials by using two-dimensional materials with negative correlation between electrical and thermal conductivity', *Nature Communications*, 7(1). doi:10.1038/ncomms12011.

[3] Sawahata, H. et al. (2023) 'First-principles calculation of Anomalous Hall and Nernst conductivity by local Berry phase', *Physical Review B*, 107(2). doi:10.1103/physrevb.107.024404.

Electron microscopy study of Zr oxides coating effect on charge-discharge properties of LiCoO₂ cathode for lithium-ion batteries

Takafumi Takeya¹, Kohei Aso¹, Hiroki Ito², Sho Asano², Yoshifumi Oshima¹ and Masaaki Hirayama²

¹ Japan Advanced Institute of Science and Technology, Ishikawa 923-1292

² Tokyo Institute of Technology, Kanagawa, 226-0026

Understanding cathode materials is important for the lithium (Li)-ion battery with higher performance. A layered rock salt-type structure material is widely used for the cathode, in which Li ions are arranged between the layers of metal oxide. A typical example is lithium cobaltite (LiCoO₂, LCO). LCO is generally used in the range of 4.2 V (vs. Li/Li⁺) or lower, where there is no significant decrease in capacity after charge-discharge cycles. If the cycle is repeated at higher potentials, the crystal structure of LCO is irreversibly changed, and the capacity fade occurs. However, if LCOs can be used stably at higher potentials, more Li ions can be used in the battery reaction, contributing to higher battery capacity.

Recently, it has been reported that capacity fade under high potential can be reduced by coating the cathode surface with metal oxide [1]. However, most metal oxides have low electron and ion conductivity, and excessive coating seems to lead to a decrease in the Li deintercalation and intercalation reaction rate. A more detailed understanding of such coating effect requires clarifying local information such as what size and how the oxide is present at the interface between the LCO cathode and electrolyte. Since polycrystalline electrodes contain conductive additives and binding agents, making the interfacial phenomena complex, it isn't easy to clarify the coating effect at the interface.

In this study, we fabricated the epitaxial LCO film as a cathode for obtaining an uncomplicated interface with electrolyte and modified the surface of the LCO film by coating Zr oxide. To observe the cross-section of the sample, the observed sample was obtained by the focused ion beam. The samples were observed using a scanning transmission electron microscope (STEM).

The cathode consisting of SrRuO₃ current collector and LCO active material was synthesized by pulsed laser deposition (PLD) on SrTiO₃(111) substrate. Li₂ZrO₃ was used as the Zr oxide target. Two types of Zr-coated samples were synthesized: a Li₂ZrO₃ deposited after LCO deposition (LZO/LCO) and an alternately deposited sample (Zr-LCO). A pure LCO sample was also synthesized for comparison. STEM was used for analysis. Charge-discharge measurements were performed by incorporating the thin cathode into a coin cell. A Li metal foil was used as an anode. The electrolyte solution was a mixture of ethylene carbonate and diethyl carbonate at a volume ratio of 3:7 with 1 M LiPF₆ dissolved as the supporting electrolyte. The potential cycling test was conducted at a 1C rate and a cutoff potential of 2.8-4.5 V.

References:

[1] H. Zhou, et al., *Advanced Energy Materials*, volume 13, issue 44, page 2302402 (2023)

Enhancing Rashba Spin-Orbit Coupling by Engineering Superlattice Interfaces of Light-Element Metal

Yusuf Wicaksono¹, Koichi Kusakabe², Seiji Yunoki³, Sadamichi Maekawa^{3,4,5}

¹ RIKEN Cluster for Pioneering Research (CPR), 2-1 Hirosawa, Wako, Saitama 351-0198, Japan.

² School of Science, Graduate School of Science, University of Hyogo 3-2-1 Kouto, Kamigori-cho, Ako-gun, 678-1297, Hyogo, Japan

³ Computational Quantum Matter Research Team, RIKEN Center for Emergent Matter Science (CEMS), Wako, Saitama 351-0198, Japan

⁴ Kavli Institute for Theoretical Sciences, University of Chinese Academy of Sciences, Beijing 100190, China

⁵ Advanced Science Research Center, Japan Atomic Energy Agency, Tokai 319-1195, Japan

The Rashba effect is a type of spin-orbit (SO) splitting that occurs on surfaces and interfaces where the inversion symmetry is broken. The two main contributions to creating large Rashba SO spin splitting are a strong atomic SO coupling (SOC) interaction and an internal electric field along the surface/interface normal. Rashba SOC strength is commonly improved by introducing materials based on heavy elements, such as those found in Bi on the Ag(111) or BeTeI surface, resulting in $\alpha_R = 3.05$ and 4.30 eV\AA [1,2]. On the other hand, creating Rashba SOC as high as those of heavy-element-based materials in nonheavy-element materials while optimizing the internal electric field has been challenging. In this study, we propose a new strategy to amplify the spin-orbit coupling effect on simple light elements metal of Cu/Cu₃N generating a massive Rashba SOC to $\alpha_R = 3.80 \text{ eV\AA}$, from optimizing the internal electric field that comes from the polarity, interface, and superlattice structure. Our proposal was confirmed through first-principles calculations. This strategy provides a powerful way to design the next generation of spintronics without the use of heavy components.

References:

[1] C. R. Ast et al., Giant spin splitting through surface alloying, Phys. Rev. Lett. 98, 186807 (2007)

[2] M. Sakano et al., Strongly spin-orbit coupled two-dimensional electron gas emerging near the surface of polar semiconductors, Phys. Rev. Lett. 110, 107204 (2013).

Figures and captions

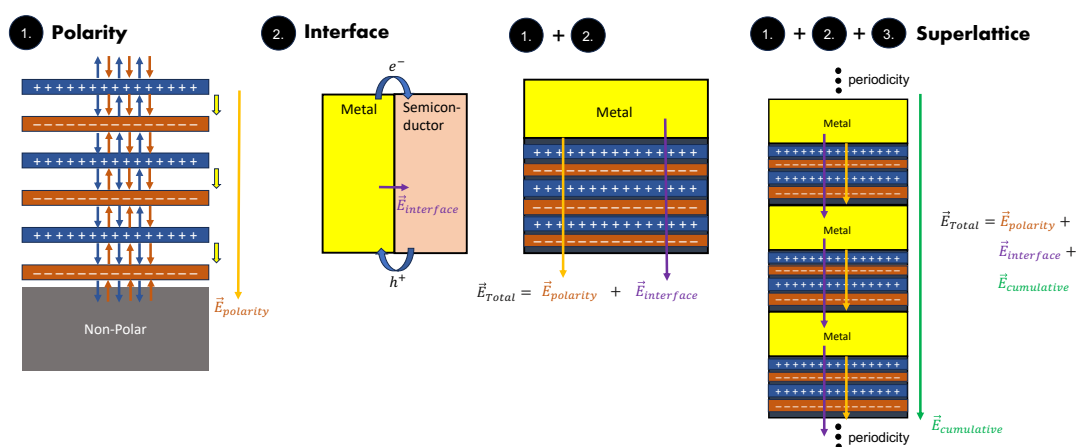


Figure 1. The strategy to optimize the internal electric field to create giant Rashba SOC on light-element-based materials through engineering the interfaces of the superlattice structure.

Enabling visible-light-charged near-infrared persistent luminescence in organics by intermolecular charge transfer

(Japan Advanced Institute of Science and Technology) ○Lin Cunjian, Jumpei Ueda
(Xiamen University) Wu Zishuang, Yang Rujun, Zhuang Yixi, Xie Rong-Jun
(Shanghai University) Xu Jie

Abstract Visible light is a universal and user-friendly excitation source but charging persistent luminescence (PersL) with visible light remains highly challenging. Herein, the concept of intermolecular charge transfer (xCT) is applied to a typical host-guest molecular system, which allows for a much-lowered energy for charge separation and enables efficient charging of near-infrared (NIR) PersL in organics by visible light ranging from 380 to near 650 nm. The NIR organic PersL is obtained by trapping electrons from charge transfer aggregates (CTAs) into constructed trap states with trap depths from 0.63 to 1.17 eV and detrapping these electrons with thermal stimulation, leading to a unique light storage effect and long-lasting emission up to 4.6 hours at room temperature. By varying the electron-donating ability in a series of acenaphtho[1,2-*b*]pyrazine-8,9-dicarbonitrile-based CTAs, the xCT absorption range is modulated and the organic PersL can be tuned from 681 to 722 nm. This study on NIR organic PersL based on xCT interactions may provide a major step forward understanding the underlying luminescent mechanism of organic semiconductors and expanding their applications in optoelectronics, energy storage, and medical diagnosis.

Results and discussion

- (1) The excitation wavelength, ranging from 380 to near 650 nm, facilitated efficient charge separation in the luminescent center. This provides a substantial advantage in charging energy compared to one of the best records inorganic NIR PersL phosphor, $\text{ZnGa}_2\text{O}_4:\text{Cr}^{3+}$.
- (2) The NIR PersL in a pTAP@TPBi film lasts for more than 4 hours at room temperature, still leaving additional energy stored at room temperature for over 1 month. This sets a new record for the longest NIR PersL duration in organics.
- (3) We first realized a trap depth exceeding 1.0 eV under various visible light excitation in organic host-guest materials through experimental and theoretical results. The trap state, comprising the LUMO of the host radical anion and that of the guest radical anion, endows the materials with the capacity to store separated charge carriers.
- (4) It was found that the trap depth and emission wavelength of the materials are controllably manipulated via regulating electron donating segments of the guest.
- (5) Regarding the exceptional light energy storage of organic materials, we first pioneered triple-mode NIR anti-counterfeiting using a mobile phone flashlight and implemented information storage via a blue laser direct writing method.

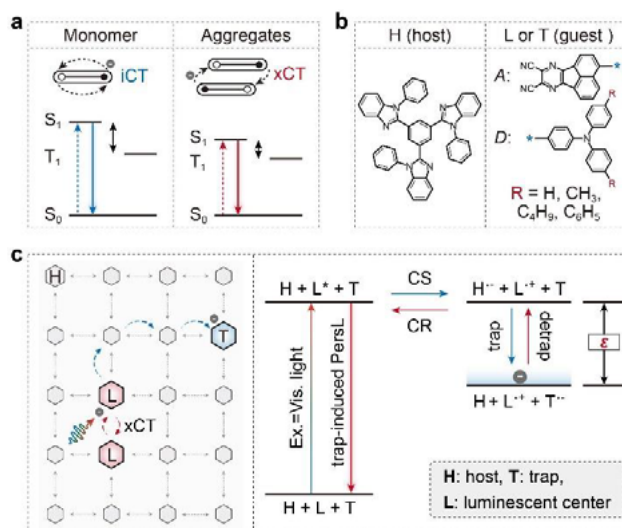


Figure 1 | PersL based on xCT process in a host-guest molecular system. **a**, Schematic illustration of the energy levels of guest monomers (left) and aggregates (CTAs, right). Compared to those in monomers, the energy difference between the excited state (S_1/T_1) and ground state (S_0) is lowered in aggregates due to the xCT process, which allows for efficient charge separation under light irradiation at a longer wavelength. **b**, Chemical structure of TPBi as the host molecule (left) and AP-based TADF molecules as the guest (right). **c**, Schematic illustration of the possible PersL mechanism in organics based on xCT interaction. The left shows electron migration in a host-guest structure model and the right depicts the electron migration process in a proposed energy-level diagram. Briefly, electrons from CTAs can be excited under irradiation of visible light and captured by traps. The trapped electrons are released under thermal stimulation, recombine with the CTAs and finally give PersL.

